Award Accounts
The Chemical Society of Japan Award for 2006

Structure and Function of Molecular Assembly.
A Personal Reminiscence

Yasuhiro Aoyama[†]

Department of Synthetic Chemistry and Biological Chemistry, Graduate School of Engineering,
Kyoto University, Katsura, Nishikyo-ku, Kyoto 615-8510

Received December 9, 2008; E-mail: aoyamay@sbchem.kyoto-u.ac.jp

In this account is described an outline of research the author has conducted over the last 35 years. Depending on the type of molecular assemblies dealt with, the whole work is divided into four parts, i.e., small host–guest systems in organic media, infinite solid systems, huge but finite nano systems in aqueous media, and manipulated biological systems. The essence of the host–guest systems (Section **2**) is molecular recognition based on convergent multiple interactions involving O–H⋯O hydrogen bonds, where sugar binding and detailed thermodynamic analysis of multipoint recognition may be taken as highlights. A couple of new fields arise from the host–guest chemistry by paradigm shift. One is in the direction of multiple interactions, from convergent to divergent. Section **3** thus concerns molecular alignment control in crystals using orthogonal aromatic triad and diad building blocks. Catalysis by microporous metallo-organic frameworks as organic zeolites is also described. The other shift in paradigm is in the media, from organic to aqueous, and also in the significance of sugar binding, from sugars as a guest to sugars as a probe. Section **4** is devoted to the highly adhesive (hydrogen bonding) nature of glycocluster compounds and their micelle-like aggregates, focusing on the formation of glycoviruses and glycoviral gene delivery. With DNA and RNA manipulation techniques in hand, we became interested in in-cell gene sensing and transcription monitoring. The latest activity in this area is shown in Section **5**. The entire work is design-based. The author, who is soon retiring from Kyoto University, now has mixed feelings about this apparently natural approach, as briefly referred to in the Closing Remark (Section **6**).

1. Introduction

The term molecular assembly is often referred to in conjunction with intermolecular order. As such, it is now a key concept in all areas of chemical science and technology. Even a synthetic chemist cannot be free from that, since the transition state of an intermolecular reaction is nothing other than a molecular assembly. Molecular assemblies are hierarchical, where the topology of unit intermolecular interactions at the bottom governs the structure and hence function of the resulting assemblies at the top. Topology control may thus be a primary concern.

The present account is a personal reminiscence of my research over the last 35 years. I have so far been involved in apparently various areas, which are linked together with molecular assembly and hydrogen bonding as key issues. Looking back into the whole work, there seems to be another or hidden key word. This is size. Accordingly, this account is divided into four parts, i.e., small host–guest systems in organic

media, infinite solid systems, huge but finite nano systems in aqueous media, and manipulated biological systems. I have often changed my research subjects. I will particularly try to describe why and how I did so.

2. Host–Guest Systems with Convergent Multiple Interactions in Organic Media

2.1 Acid–Base Cooperation. Physical organic chemistry was one of the most active areas of chemistry when I started my academic carrier in 1968. My research subject in undergraduate and graduate courses at Kyoto University was structure–reactivity correlation in free radical substitution reactions. Upon finishing my doctoral work under the supervision of Prof. I. Tabushi, I got a position as a research associate at Kyushu University. In the laboratory of Prof. Y. Murakami, I was involved in the rapidly growing bioorganic and -inorganic fields, mostly dealing with enzyme mimics. If one paper is to be referred to here, I would like to cite a piece of work on macrocyclic enzyme models.[1] Deacylation of fatty acid *p*-nitrophenyl ester is facilitated by [20]paracyclophane oxime **1a** (Chart 1) as a host in alkaline aqueous media. Pre-equilibrium binding of the substrate with the host via hydrophobic forces is followed by nucleophilic attack of the oxime nucleophile on

---

† Present address: Department of Molecular Chemistry and Biochemistry, Faculty of Science and Engineering, Doshisha University, 1-3 Tatara Miyakodani, Kyotanabe, Kyoto 610-0321

the ester moiety of the bound substrate. We introduced a charged group on the benzene ring (compounds **1b** and **1c**). The deacylation (actually acyl transfer from the substrate to the host) is greatly accelerated by the positively charged ammonium group (**1b**) or seriously decelerated by the negatively charged carboxylate group (**1c**). The observed charge effect is understandable in terms of nucleophilic–electrostatic bifunctional cooperation; the negative charge developing in the substrate at the transition state of nucleophilic attack is electrostatically either stabilized by the positive charge or destabilized by the negative charge, as schematically shown in structure **2** for the ammonium stabilization case.

In January of 1981, I moved to snow-covered Nagaoka (Nagaoka University of Technology) as an associate professor to join the group of Prof. H. Ogoshi, where the major research subject was porphyrin chemistry. Being also encouraged by Prof. Ogoshi, I tried to start new subjects and spent much time thinking of new themes but actually I could not start, and I remained in the porphyrin area. One day, Prof. Ogoshi told me of a curious observation he had been concerned about. Compound **4**, a Rh^{III} porphyrin with ClO$_4^-$ as a noncoordinating counter anion, obtained from the corresponding Rh^{III}–Cl species **3** (Scheme 1), affords a small amount of organometallic phenyl–Rh^{III} species **5** when subjected to chromatographic purification with benzene as eluant. This note of Prof. Ogoshi
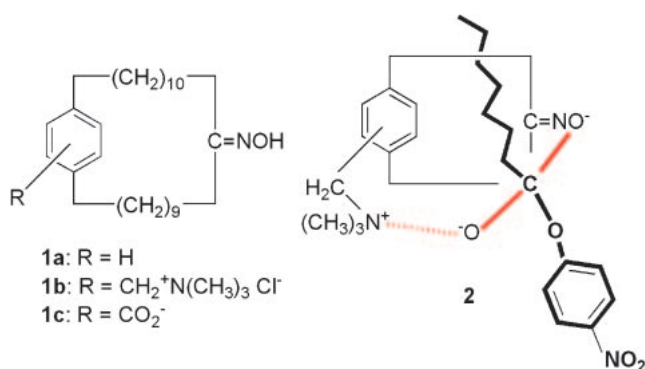
turned out to be the very start of my research which, in a sense, has been continuing up to now. I was simply impressed by the electrophilicity of the cationic Rh^{III} of concern, being capable of direct aromatic substitution (metallation) (Scheme 1). We elucidated the complete details of this electrophilic aromatic metallation with Hammett-type substituent correlation.[2]

We then switched to acetone, which readily gave the corresponding organometallic compound **6** presumably via enolization of the ketone with Rh^{III} as an acidic promoter and a base (formally ClO$_4^-$) to abstract a proton (Scheme 1). The cationic Rh^{III} is essential as a promoter, since the chlororhodium derivative **3** shows no activity at all. We formulated the present Rh^{III}-promoted C–H activation in terms of superelectrophilicity or super-Lewis acidity of the cationic Rh^{III} porphyrin **4**. A little concern was the identity of the base. Is it really ClO$_4^-$? One day, it occurred to me that even the less electrophilic and hence otherwise inactive Rh^{III}–Cl porphyrin **3** may work when an appropriate base is available in the vicinity of the metal center. This was indeed the case. In marked contrast to the corresponding dinaphthyl derivative, the Rh^{III}–Cl compound of diquinolylporphyrin **7** immediately gives rise to the C–Rh^{III} compound **8** supposedly via cooperation of the Rh^{III}–Cl center as a weak Lewis acid and the quinolyl nitrogen as a Brønsted base (Scheme 2).[3] Essentially, the coordination axis to the Rh^{III} center (acid) and the direction of lone-pair electrons on the nitrogen (base) are perpendicular to each other as shown by arrows in structure **7**, so that neither intramolecular nor intermolecular acid–base neutralization takes place, the respective acid and base activities being thus preserved.

2.2 Two-Point Fixation of Bifunctional Guests. The concerted acid–base cooperation shown in Scheme 2 is a mechanistic explanation and, as a transition-state phenomenon, is not directly verifiable. If such a cooperation indeed occurs at the transition state, why could not we expect similar multiple interactions in the ground state? Thus, we were naturally led to visualization of multiple interactions as a ground-state phenomenon, i.e., in the host–guest complexation, where respective interactions must be reflected on the binding constants of

Chart 1. Structures **1** and **2**.
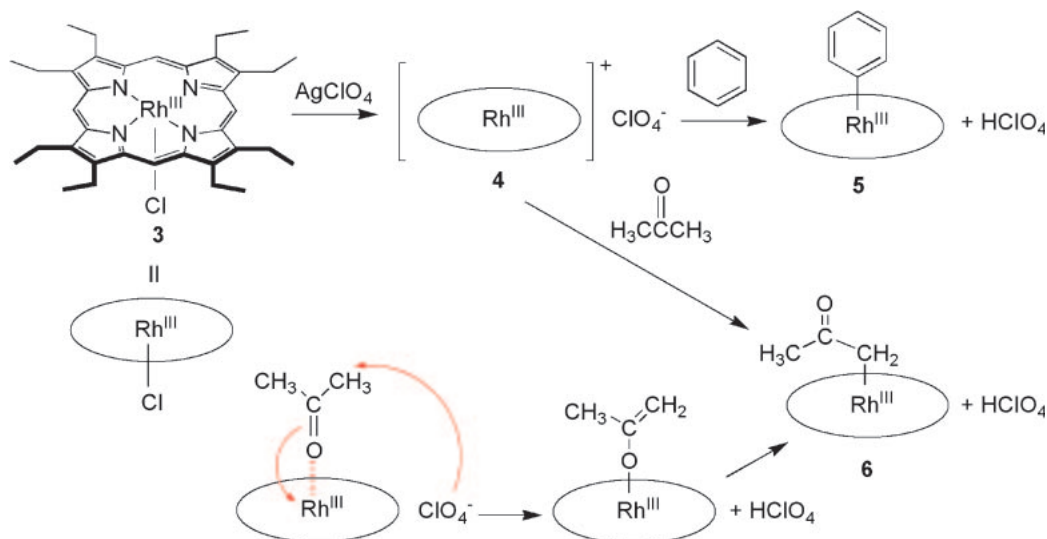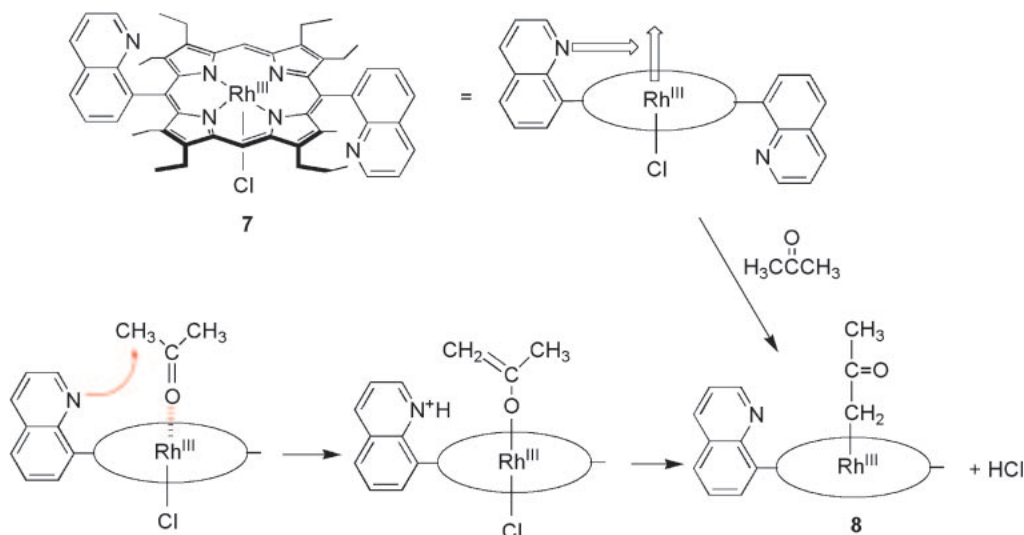
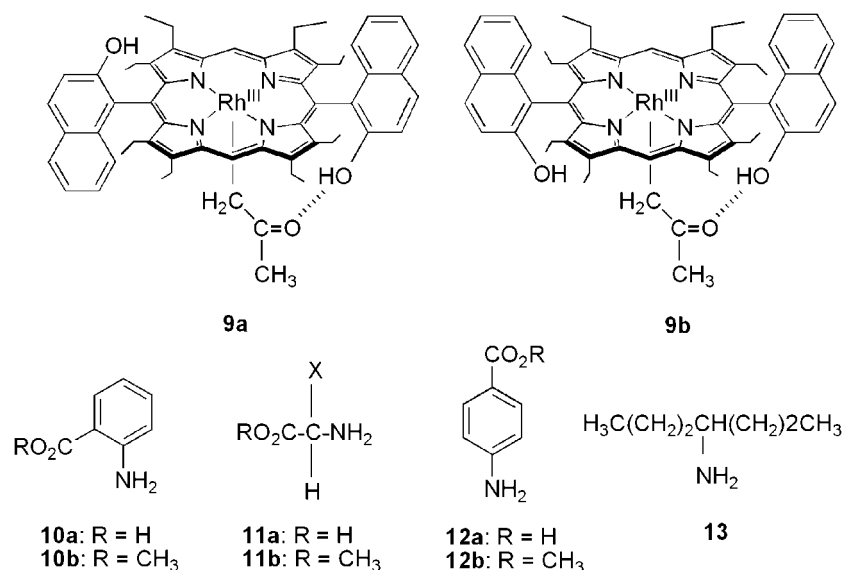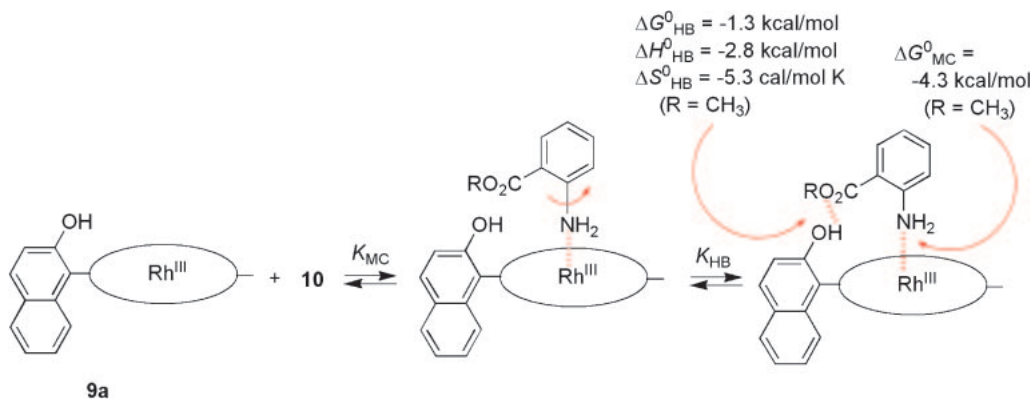**Scheme 1.**

Scheme 2.

Chart 2. Structures **9**–**13**.

the host–guest complexes and also hopefully be confirmed directly by X-ray crystallography.

A naphthol-functionalized Rh^{III} porphyrin (acetone-coordinated *trans*-dinaphthol derivative **9a** (Chart 2)) as a host (H) reversibly binds amino acids (*o*-aminobenzoic acid (**10a**) and α-amino acids (**11a**)) and their methyl esters **10b** and **11b** as a guest (G) in chloroform via simultaneous metal-coordination ($Rh^{III}\cdots NH_2$) and hydrogen-bonding ($OH\cdots CO_2R$; R = H or CH_3) interactions, as shown in Scheme 3 for the binding of guest **10**.[4a,4b] The corresponding *cis*-dinaphthol derivative **9b** having no OH group in the open coordination side serves as a reference host (rH) capable of only metal coordination. *p*-Aminobenzoic acid/ester **12a** and **12b** and simple amine **13**, on the other hand, serve as reference guests (rG) free from hydrogen bonding. Our primary concern is to fully characterize the weaker interaction, i.e., hydrogen bonding. The significance of this interaction may be easily recognized by referring to the selectivity for the two-point adduct over the one-point counter-

part, i.e., $K_{HG}/K_{rHG} = 11.3$ or $K_{HG}/K_{HrG} = 6.1$ for *o*-aminobenzoic ester **10b** (G) in chloroform at 288 K (rG = *p*-aminobenzoic ester **12b**) or more precisely to the corrected selectivity $K_{HB} = (K_{HG}/K_{rHG})/(K_{rHrG}/K_{rHrG}) = (K_{HG}/K_{HrG})/K_{rHG}/K_{rHrG} = 9.50$ and $\Delta G^0_{HG} = RT \ln K_{HB} = -1.3 \text{ kcal mol}^{-1}$ ($1 \text{ kcal mol}^{-1} = 4.184 \text{ kJ mol}^{-1}$) ($\Delta H^0_{HG} = -2.8 \text{ kcal mol}^{-1}$ and $\Delta S^0_{HG} = -5.3 \text{ cal mol}^{-1} \text{K}^{-1}$ obtained from variable-temperature measurements). The contribution of metal coordination is $K_{MC} = K_{HG}/K_{HB} = 1.86 \times 10^3 \text{ M}^{-1}$ ($1 \text{ M} = 1 \text{ mol dm}^{-3}$) and $\Delta G^0_{MC} = RT \ln K_{MC} = \Delta G^0_{HG} - \Delta G^0_{HB} = -4.3 \text{ kcal mol}^{-1}$ (288 K). In this way, the total binding free energy of $\Delta G^0_{HG} = -5.6 \text{ kcal mol}^{-1}$ is separated into two contributors, ΔG^0_{HG} and ΔG^0_{MC}, as shown in Scheme 3 for the two-point fixation of guest **10b**. The hydrogen bonding becomes more pronounced in going from ester **10b** to carboxylic acid **10a** as a guest; for the latter $K_{HB} = 107$ ($\Delta G^0_{HG} = -2.7 \text{ kcal mol}^{-1}$) and $K_{MC} = 1.12 \times 10^3 \text{ M}^{-1}$ ($\Delta G^0_{MC} = -4.0 \text{ kcal mol}^{-1}$) (288 K). While the hydrogen bonding even in the

$\Delta G^0_{HB} = -1.3$ kcal/mol
$\Delta H^0_{HB} = -2.8$ kcal/mol
$\Delta S^0_{HB} = -5.3$ cal/mol K
(R = CH$_3$)

$\Delta G^0_{MC} = -4.3$ kcal/mol
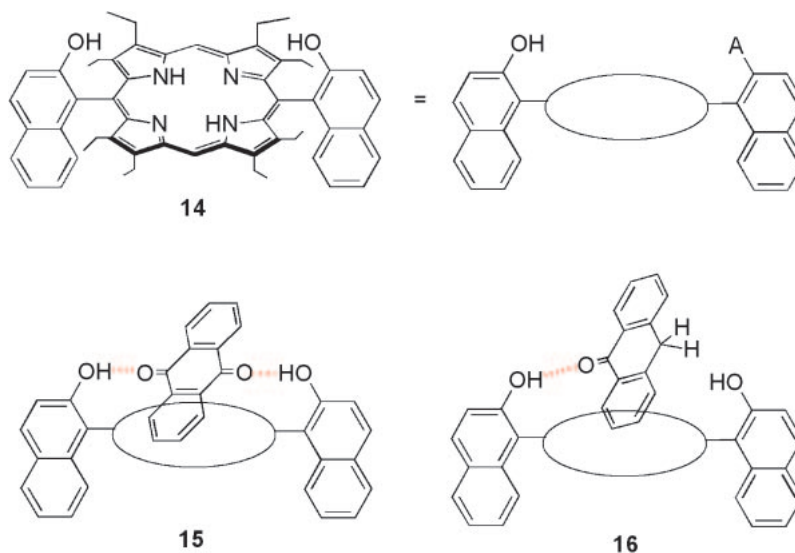(R = CH$_3$)

Scheme 3.

Chart 3. Structures **14**–**16**.

carboxylic acid system is much weaker than the metal coordination, the former does bring about a sizable selectivity.

The formation of a two-point adduct may be assumed, from a thermodynamic point of view, to proceed via a hypothetical one-point metal-coordinated adduct (Scheme 3), where the equilibrium constants for the initial intermolecular association and subsequent intramolecular conformational fixation correspond respectively to the parameters K_{MC} and K_{HB} referred to above. The thermodynamic parameters associated with the latter (hydrogen bonding) process for the binding of amino ester **10b** ($\Delta H^0_{HG} = -2.8$ kcal mol^{-1}, $\Delta S^0_{HG} = -5.3$ cal mol^{-1} K^{-1}, $\Delta G^0_{HG} = -1.3$ kcal mol^{-1}, and $K_{HB} = 9.50$; Scheme 3) may be compared with those for the intermolecular hydrogen-bonding fixation of methyl acetate to the present naphthol host **9a**; $\Delta H^0_{HG} = -2.4$ kcal mol^{-1}, $\Delta S^0_{HG} = -10.2$ cal mol^{-1} K^{-1}, $\Delta G^0_{HG} = 0.56$ kcal mol^{-1}, and $K_{HB} = 0.38$ M^{-1} (288 K). The enthalpy changes are reasonably similar to each other. It is in the entropy changes that the two processes are markedly different from each other. The entropy cost for the intramolecular fixation of pre-bound guest is significantly lower than that for the intermolecular complexation of free guest in solution ($\Delta\Delta S^0 = 10.2 - 5.3 = 4.9$ cal mol^{-1} K^{-1} or $T\Delta\Delta S^0 \cong 1.5$ kcal mol^{-1} at 298 K (we will get back to this point later in Section **2.4**). In this way,

the otherwise inefficient hydrogen bonding gives rise to a net gain in free energy when incorporated in a multiple interaction.[4b]

Another good example of multiple interaction is the two-point hydrogen-bonding fixation of quinones.[5] Anthraquinone, for example, is bound to a *cis*-bis(hydroxynaphthyl) derivative of porphyrin **14** in this manner (**15**) with $K = 2.3 \times 10^2$ M^{-1} (chloroform, 298 K), as compared with $K = 4.2$ M^{-1} for anthrone which only forms one-point adduct (**16**) (Chart 3).

2.3 Calix[4]resorcarene as a Multiple O–H⋯O Hydrogen-Bonding Host. While the rigid porphyrin framework with an ideal geometrical arrangement provided a novel model system to characterize the two-point interactions, we had to go further beyond this model case. For this and other reasons, I decided to leave the porphyrin chemistry when I was promoted to a full professor in Nagaoka in 1988. In those days, hydrogen bonding was receiving more and more attention in the area of molecular recognition. Most scientists in this field were concerned about nitrogen-based hydrogen bonds of the type N–H⋯N or N–H⋯O (N⋯H–O). This appears reasonable since nitrogen is generally more basic than oxygen on the one hand and on the other, the hydrogen bonds maintaining the structure and function of nucleic acids and proteins are all of this type. If so however, why should not we go to the unexplored O–H⋯O system.
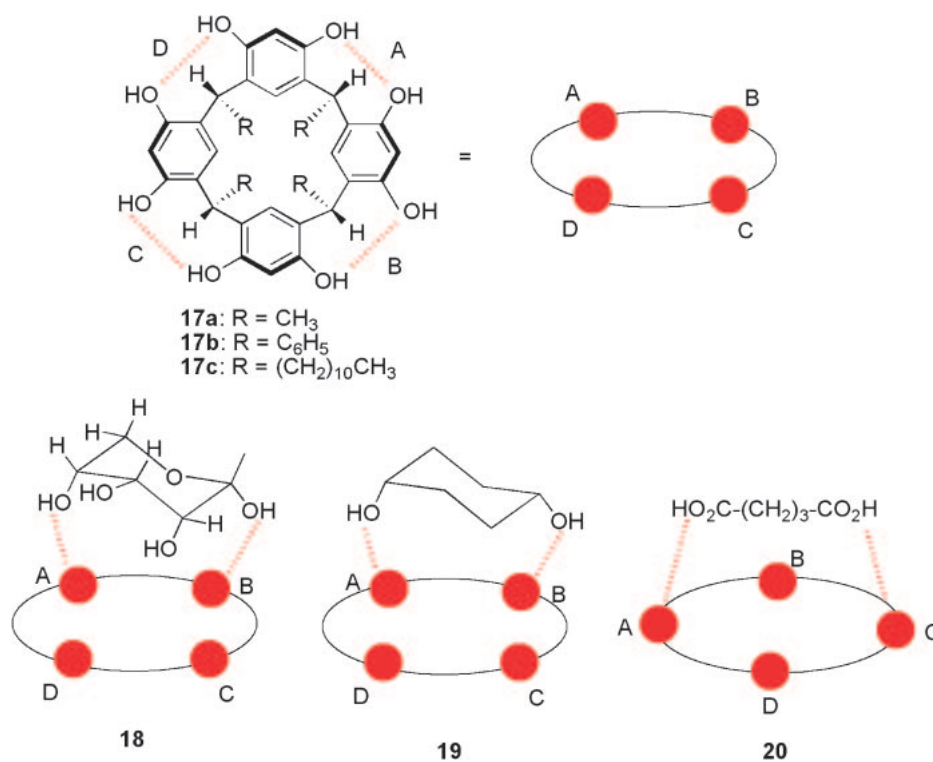
Chart 4. Structures **17–20**.

Accidentally, we had already dealt with this type of hydrogen bond in the binding of amino acids and quinones as shown above. Furthermore, there are a variety of important oxygen compounds such as sugars that may serve as intriguing targets or guests. A new subject started in this way. We spent time to design host molecules for this purpose, but it was not an easy task for me. It was Y. Tanaka, a graduate student in my group at that time, who noticed the potential utility of the resorcinol–aldehyde cyclic tetramer **17** (hereafter called calix[4]resorcarene) (Chart 4). Derivatives of this compound derived from acetaldehyde (**17a**) or benzaldehyde (**17b**) have long been known, but they are soluble neither in water nor in common organic media. Mr. Tanaka used a long-chain aldehyde, actually dodecanal, to solve the solubility problem. The idea worked nicely. The resulting resorcinol–dodecanal cyclic tetramer **17c** was readily soluble even in CCl₄. We got excited when we found that host **17c** in chloroform could extract ribose, a pentose sugar, as a guest from an aqueous solution on a 1:1 (host to guest) basis.[6a] Subsequently, we were convinced of some sort of specific host–guest complexation taking place, when we noted that ribose was bound almost exclusively in the α-pyranose form rather than the more stable β-anomer.[6b]

Molecular recognition of oxygen compounds such as sugars,[6,7] carboxylic acids,[8] alcohols,[7,9] steroids,[7] and glycosides[10] started in this way and created a new field of host–guest chemistry. Despite its apparent structural similarity to calixarenes, calix[4]resorcarene **17c** is actually far from analogous to the former. Calix[4]resorcarene is what may be called a tetradentate host having four independent binding sites composed of a pair of hydrogen-bonded OH groups (O–H⋯O–H)[11] that serve as a unit hydrogen-bonding site for a polar functional group such as C=O of the guest (O–H⋯O–H⋯O=C). The four
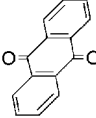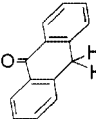
sites A, B, C, and D, referring to structure **17**, are located at a distinct distance. This must give rise to selectivity in the binding of multifunctional guests. Evidence shows that ribose is bound highly stereoselectively as α-pyranose which possesses 1-OH and 4-OH groups in a cis configuration to allow their simultaneous hydrogen-bonding fixation with the adjacent A and B sites of the host **18**.[6b] The corresponding cis-to-trans stereoselectivity in the binding of soluble 1,4-cyclohexanediol is 8:1; $K = 1.04 \times 10^3$ and $1.29 \times 10^2\,\mathrm{M}^{-1}$ (CDCl₃, 298 K) for the cis (**19**) and trans isomers, respectively.[9] Binding of dicarboxylic acids exhibits a chain-length selectivity. The strongest binding occurs at glutaric acid HO₂C(CH₂)₃CO₂H with $K = 1 \times 10^5\,\mathrm{M}^{-1}$ (CDCl₃), which is 2-orders or 3-orders of magnitude larger than that for pimelic acid HO₂C(CH₂)₅-CO₂H ($K = 1.1 \times 10^3\,\mathrm{M}^{-1}$) or valeric acid CH₃(CH₂)₃CO₂H ($K = 7 \times 10\,\mathrm{M}^{-1}$) as long dicarboxylic and monocarboxylic acid references.[8] Models suggest that glutaric acid best fits for the two-point fixation with the diagonal binding sites A and C (**20**).

2.4 Generalization of Entropic Preference in Multiple Interactions. For the sake of thermodynamic analysis, let us apply the stepwise mechanism once again (Scheme 4a); formation of a two-point adduct involves initial intermolecular complexation to give a one-point adduct, which then collapses into the two-point adduct. For the combination of symmetric host **17c** or **14** and symmetric or quasi symmetric guest (glutaric acid, 1,4-cyclohexanediol, or anthraquinone), the strengths (ΔH^0) of hydrogen bonds at both sites (referring to **15**, **19**, and **20**) are the same or nearly the same and may also be assumed to be the same as that for the binding of one-point reference guest (Scheme 4b). It is in entropy that the intermolecular and intramolecular processes differ
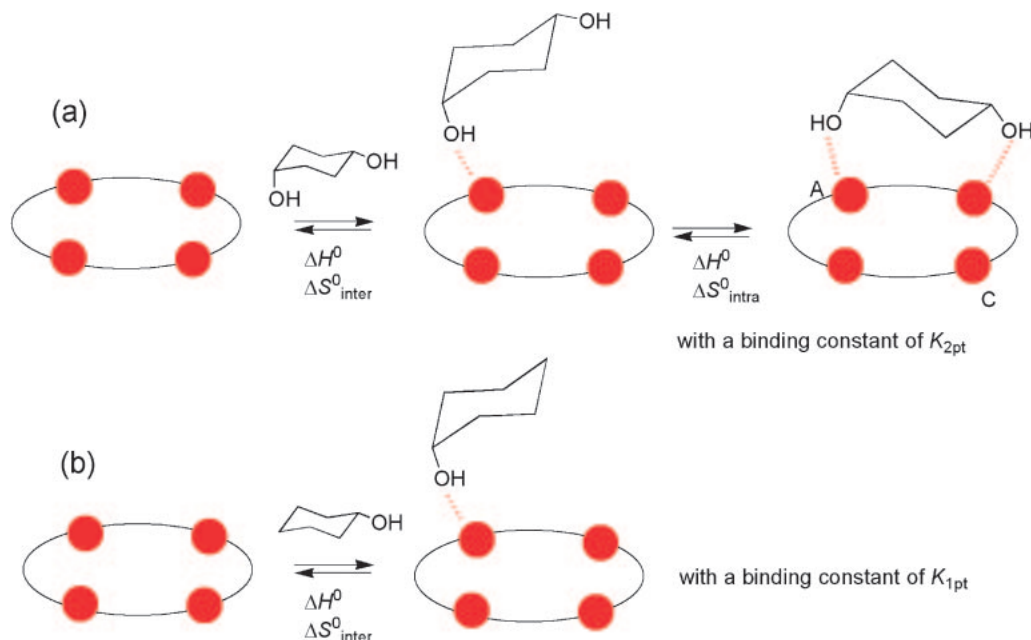
Scheme 4.

Table 1. Binding Constants for Host–Guest Complexation in Chloroform

	Guest		
	anthraquinone	*cis*-1,4-cyclohexanediol	$HO_2C-(CH_2)_3-CO_2H$
K_{2pt}/M^{-1}	230	1040	1×10^5
	Guest		
	anthrone	cyclohexanol	$CH_3-(CH_2)_3-CO_2H$
K_{1pt}/M^{-1}	4.2	11	1×10^2
K_{2pt}/K_{1pt}	55	95	10^3
$K_{2pt}/(K_{1pt})^2$	13	8.9	10

from each other. The entropy change (ΔS^0_{intra}) associated with the second step (intramolecular) in the two-point fixation must be less unfavorable than that (ΔS^0_{inter}) for the first step (intermolecular); the latter could again be assumed to be the same as that for the intermolecular binding of reference guest. The total free energy change for the two-point fixation is $\Delta G^0 = (\Delta H^0 - T\Delta S^0_{inter}) + (\Delta H^0 - T\Delta S^0_{intra}) = 2\Delta H^0 - T(\Delta S^0_{intra} + \Delta S^0_{intra})$.

The respective binding constants K_{2pt}, already referred to above as K, for the two-point fixation of anthraquinone (with porphyrin host **14**), *cis*-1,4-cyclohexanediol (with calix[4]-resorcarene host **17c**), and glutaric acid (with **17c**) are summarized in Table 1, together with those (K_{1pt}) for the corresponding monofunctional reference guests, i.e., anthrone, cyclohexanol, and valeric acid, respectively. There is a big span

(ranging in the order of 10^2 to 10^5) in the stabilities (K_{2pt}) of the two-point adducts. The apparent two-point/one-point selectivities (K_{2pt}/K_{1pt}) also change from 55 through 95 to 10^3. It is impressive on the other hand, to note that the term $K_{2pt}/(K_{1pt})^2$ remains nearly constant at 10. In terms of free energy, this corresponds to the difference between one two-point adduct and two one-point adducts; $RT\ln[K_{2pt}/(K_{1pt})^2] = RT\ln K_{2pt} - 2RT\ln K_{1pt} = -\Delta G^0_{2pt} + 2(\Delta G^0_{1pt})$. Since referring to Scheme 4 and the discussion in the preceding paragraph, $\Delta G^0_{2pt} = 2\Delta H^0 - T(\Delta S^0_{intra} + \Delta S^0_{inter})$ and $\Delta G^0_{1pt} = \Delta H^0 - T\Delta S^0_{inter}$, $RT\ln[K_{2pt}/(K_{1pt})^2] = T(\Delta S^0_{intra} - \Delta S^0_{inter})$. As noted above, $K_{2pt}/(K_{1pt})^2 \cong 10$, irrespective of the type and hence strength of the interactions. Hence, $(\Delta S^0_{intra} - \Delta S^0_{inter}) = R\ln(10) = 4.6$ cal mol^{-1} K^{-1} or $T(\Delta S^0_{intra} - \Delta S^0_{inter}) = 1.4$ kcal mol^{-1} at 298 K. They are in excellent agreement with the corresponding values of $\Delta\Delta S^0 = 4.9$ cal mol^{-1} K^{-1} and $T\Delta\Delta S^0 = 1.5$ kcal mol^{-1} (298 K) for the hydrogen bonding in the amino ester–porphyrin adducts (Section **2.2**). The advantage of multiple interaction is entropic in origin. The present generalization shows that the entropic cost for a pre-organized two-point host–guest complexation is lower than two times that for the one-point complexation by a factor of $T\Delta\Delta S^0 \cong 1.5$ kcal mol^{-1}. This is in the case of two-point complexation having one intramolecular interaction. For an *n*-point complexation, each of $(n-1)$ intramolecular interactions may save an entropy cost of ≈ 1.5 kcal mol^{-1}. The total saving in entropy would be great, while the total gain in enthalpy would basically be additive of those of constituent unit interactions.

3. Infinite Solid Systems with Divergent Multiple Interactions

3.1 Leaving the Nonaqueous Host–Guest Chemistry. With achievements on the newly developed O–H···O systems, highlighted by sugar binding and thermodynamic analysis of multiple interactions, I was lucky enough to be awarded The CSJ Award for Creative Work in 1991 and most unexpectedly a

Y. Aoyama

Bull. Chem. Soc. Jpn. Vol. 82, No. 4 (2009)   425
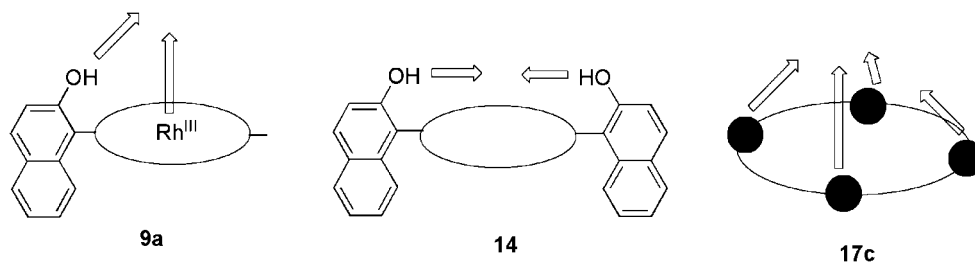
Chart 5. Structures **9a**, **14**, and **17c**.
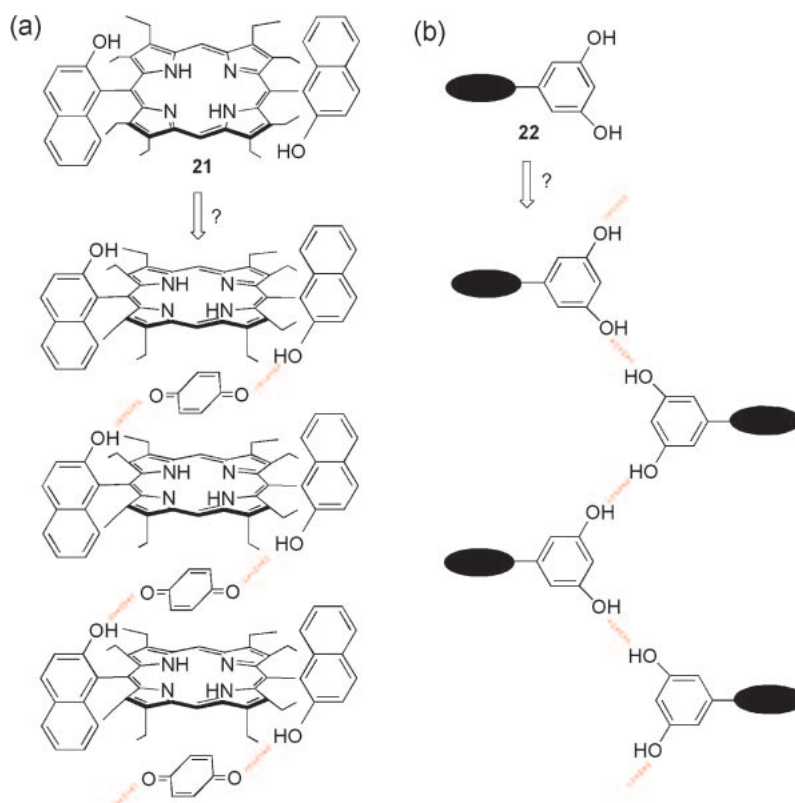
Scheme 5.

Fluka Prize (Reagent of the Year 1993). At the same time, I began to strongly feel that molecular recognition is a tool rather than an aim. Critically, the hydrogen bonds we had relied on were all in apolar organic media, mostly in chloroform, and structural order created was bimolecular at best. Nevertheless, the entropic preference of a multiple interaction must be general, since it is geometrical and should depend neither on the type of interactions nor on the polarity of the media. The principle of organization should also be common for bimolecular and multi-molecular systems. With these in mind, I decided on the occasion of the above-mentioned awarding, to leave the nonaqueous host–guest chemistry for a couple of new fields. One, with a hope to contribute to life science and technology, was polar interaction in aqueous media, as described in Section **4**. The other, with a hope to contribute to materials science and technology, was molecular alignment control in crystals, as shown below.

3.2 Orthogonal Aromatic Triads and Molecular Alignment Control.   Good multidentate hosts have convergent functional groups which simultaneously work on a guest.

Metalloporphyrin receptor **9a**, *cis*-dinaphthol **14**, and calix-resorcarene **17c** with unit interaction axes shown by arrows illustrate this point (Chart 5). *trans*-Dinaphthol porphyrin derivative **21** on the other hand, could of course not afford closed 1:1 host–guest complexes, but might still be potentially capable of forming oligomeric or polymeric 1:1 quinone–porphyrin open chains in the solid state (Scheme 5a). If a 5-substituted resorcinol **22** forms a hydrogen-bonded extended chain rather than a closed ring structure, the substituents (black ellipses) would be aligned in a columnar fashion with a predictable spacing (Scheme 5b). With these pictures in mind, we entered the crystal engineering area in the early 1990s.

It was co-worker K. Kobayashi who proposed to use anthracene–bis(resorcinol) **23** (Scheme 6) as a model building block. It is an orthogonal aromatic triad, having four divergent OH groups arranged in a symmetric manner. Recrystallization of this compound as a host from a relatively bulky ketone or ester (such as 5-nonanone, ethyl benzoate, and isobutyl acetate) as solvent affords 1:2 (host to guest) lattice inclusion complexes (guest = solvent molecule).[12] All the com-
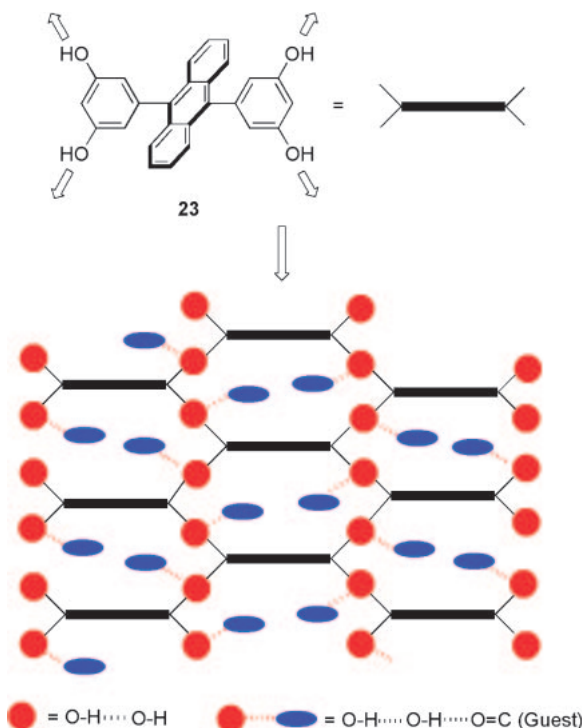
Scheme 6.

Scheme 7.

plexes examined share a common feature, the formation of a molecular sheet composed of hydrogen-bonded (O–H⋯O–H) poly(resorcinol) chains (red circles in Scheme 6 represent a pair of hydrogen-bonded OH groups (O–H⋯O–H)) and columns of orthogonal anthracene spacers (black rectangles in Scheme 6). Two guest molecules (blue ellipses in Scheme 6) are incorporated in each cavity pillared by hydrogen-bonded resorcinol rings and roofed/bottomed by the anthracene rings via host–guest hydrogen-bonding (O–H⋯O–H⋯O=C) in exactly the same manner as in homogeneous calix[4]resorcarene complexes.[12c]

The presence of intervening guest molecules was a real obstacle in constructing stacked aromatic columns. Much initial attention was paid to this issue. We made various attempts. One was to use a bifunctional guest such as anthraquinone. Adduct $23 \cdot 2$(anthraquinone)exhibits a different lattice pattern containing segregated and partially overlapped columns of antharacene (with face-to-face distance of $I^f = 5.24$ Å) and anthraquinone ($I^f = 3.03$ or 3.55 Å).[13] Another was to use anthracene–bis(pyrimidine) derivative **24** as a H-acceptor. Bis(resorcinol) and bis(pyrimidine) compounds **23** and **24** form a 1:1 cocrystal $23 \cdot 24$. The crystal structure contains a molecular sheet composed of hydrogen-bonded (O–H⋯N) poly(resorcinol–pyrimidine) chains (Scheme 7) in a similar manner as above (Scheme 6). However, the consequence of an apparently subtle change in the hydrogen-bond pattern from O–H⋯O–H to O–H⋯N is tremendous.[13] (1) The O–H⋯N hydrogen bond is coordinatively saturated and there is no guest incorporation in the cocrystal $23 \cdot 24$, in marked contrast to the case of homocrystal **23** containing coordinatively unsaturated hydrogen bonds O–H⋯O–**H** which can be rendered saturated only upon complexation of a guest molecule (O–H⋯O–**H**⋯O=C) to give inclusion complexes $23 \cdot 2G$ (G is
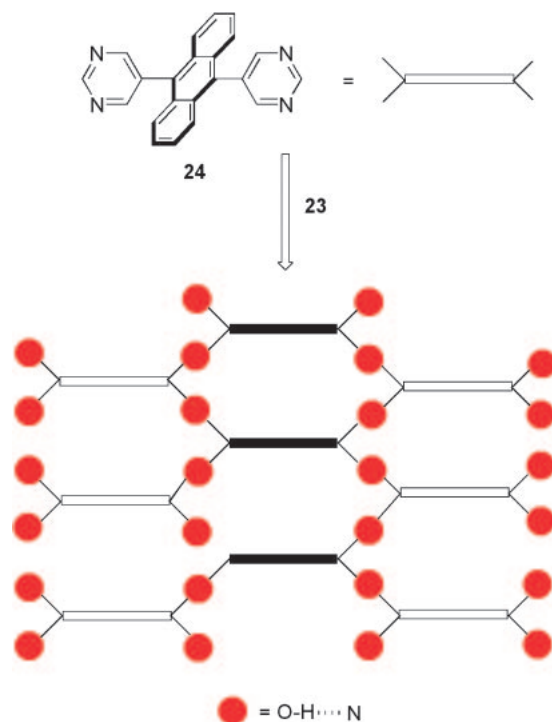
guest) (Scheme 6). (2) The N atom in the O–H⋯N hydrogen bond is a constituent of the six-membered pyrimidine ring, in contrast to the exocyclic O atom in the O–H⋯O–H hydrogen bond. As a consequence, the face-to-face distance of neighboring anthracene rings along a column in cocrystal $23 \cdot 24$ becomes significantly shorter ($I^f = 8.4$–8.5 Å), roughly by two single bonds, than that ($I^f = 12.0$–13.4 Å) in the O–H⋯O–H hydrogen-bonded inclusion complex $23 \cdot 2G$. (3) As compared with the $23 \cdot 2G$ case, neighboring sheets in cocrystal $23 \cdot 24$ come closer or interpenetrate each other in such a way as to partially fill the guest-free cavity of one sheet with the orthogonal anthracene moieties of the neighboring one. Anthracene columns of neighboring sheets become partially overlapped as a consequence.

A third approach was to use anthracene–mono(resorcinol) derivative **25** (Scheme 8), which upon recrystallization, affords 1:1 adducts $25 \cdot G$.[14] In the crystal, host **25** forms hydrogen-bonded (O–H⋯O–H) one-dimensional (1D) chains (step a), which self-assemble via interpenetration or intercalation of the orthogonal anthracene (A) moieties (step b), and such guests as duroquinone (tetramethylbenzoquinone, blue ellipse in Scheme 8) are incorporated in each cavity via hydrogen bonding as above (O–H⋯O–H⋯O=C) to give densely packed alternate $\cdots A \cdot G \cdot A \cdot G \cdots$ columns (step c). It is remarkable that many of the columns, including those described in the preceding paragraph, are constructed via self-assembly of hydrogen-bonded 1D or 2D networks.[15] The network-self-assembly strategy thus opens the door to a 3D control of aromatic columns in molecular crystals. i.e., co-alignment in the proximity of donor columns and acceptor columns.

3.3 Intracavity Reactions.   Included guest molecules are nothing other than a nuisance from the viewpoint of column construction. In view of host–guest chemistry, they are
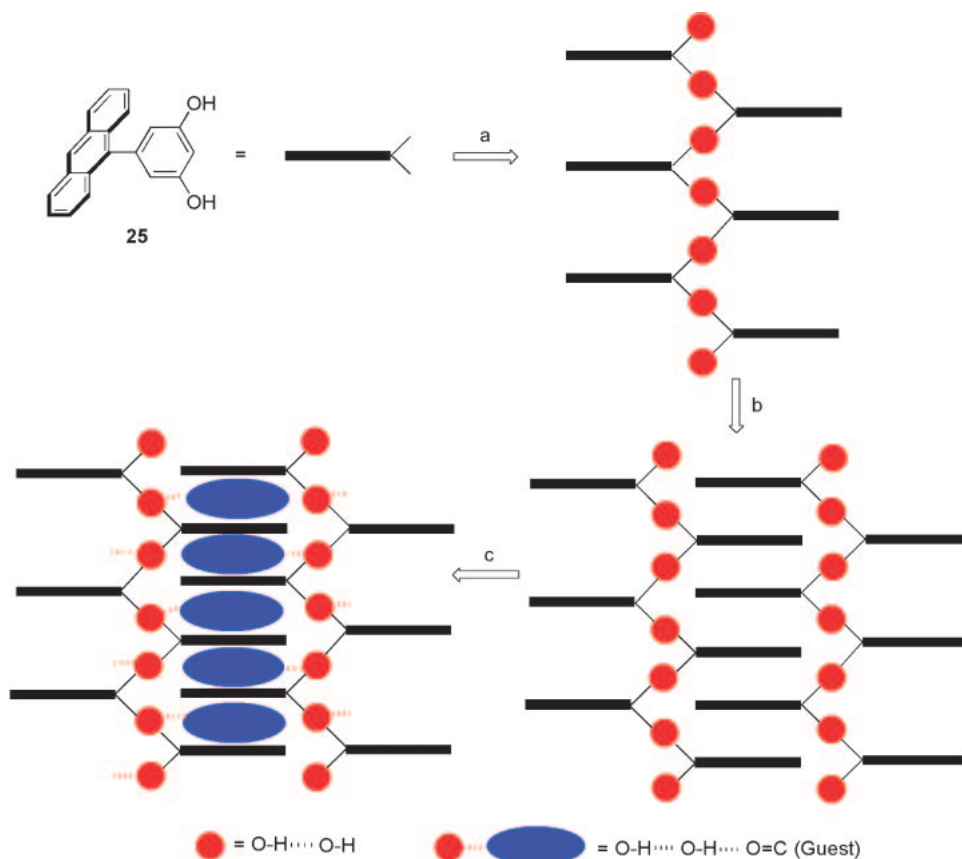
Scheme 8.
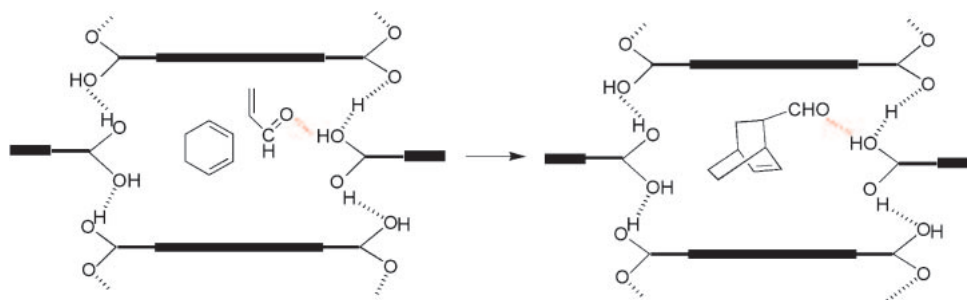
Scheme 9.

indispensable players. We were particularly interested in intracavity reactions of included guest molecules and possible catalysis thereon of the host network. The start of this work dates back to our original finding that host **23**, when recrystallized from a mixture of ethyl acetate and benzene, affords a 1:2:2 cocrystal **23**·2(CH$_3$CO$_2$CH$_2$CH$_3$)·2(C$_6$H$_6$).[12a] In light of subsequent work,[12b] it is evident that two molecules of ethyl acetate hydrogen-bonded to the host network are too small to fill the cavity and hence two molecules of benzene are picked up to occupy the remaining vacant space. The crystal structure looked as if one of the ester–benzene pairs were ready to react with each other.[12a] We changed the ethyl acetate–benzene pair to a reactive pair of acrolein or alkyl acrylate (dienophile) and 1,3-cyclohexadiene (diene) to see if host **23** could promote Diels–Alder reaction between them. This was indeed the case.

Guest-free apohost **23** (vide infra) unambiguously in the solid-state catalyzes the acrolein–cyclohexadiene Diels–Alder reaction (Scheme 9) with a catalytic cycle involving sorption of reactants into the cavity of the apohost, rate-determining intracavity Diels–Alder reaction, and partially rate-determining desorption of the product from the cavity with concomitant uptake of a new pair of reactants.[16] Apohost **23** also promotes the reaction of alkyl acrylate. Unfortunately however, it is not catalytic but stoichiometric due to product inhibition; the Diels–Alder product formed in the cavity remains there to allow no turnover behavior of the apohost. Simultaneous intracavity binding of dienophile and diene can be confirmed directly by X-ray crystallography for the 1:2:1 **23**·2(ethyl acrylate)·(1,3-cyclohexadiene) adduct at 230 K. While the acrolein–cyclohexadiene Diels–Alder reaction[16,17] and subsequent citronellal-to-isopulegol ene reaction[18] provided a novel
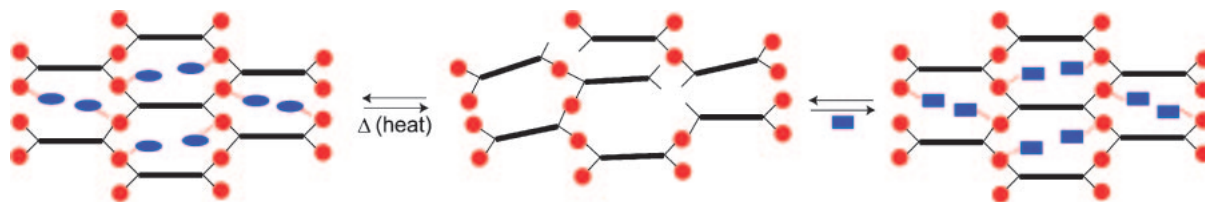
Scheme 10.
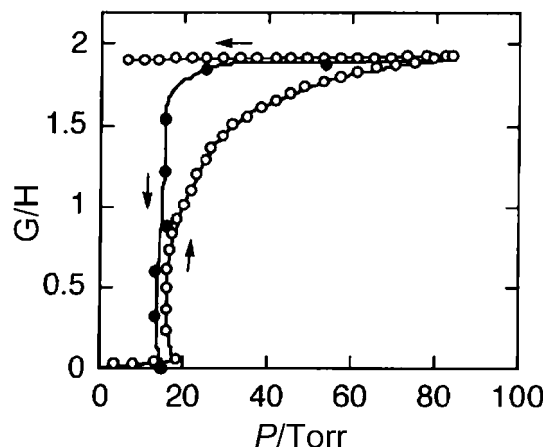
Figure 1. Binding "isotherm" for gaseous ethyl acetate with powdered apohost **23** at 25 °C under fast-scanning (○) and slow-scanning (●) conditions.

example of catalysis by "microporous" organic solids, we had to overcome the product inhibition problem to make the observed catalysis more general. Thus, we were urged to know more about dynamics and thermodynamics of lattice inclusion phenomena.

3.4 Dynamics and Thermodynamics of Lattice Inclusion Phenomena. The reluctance of included guest molecules to be desorbed is not a surprise at all but rather a necessity, since this is why the corresponding host–guest adducts **23·2G** can be isolated. Desorption of even volatile guests such as ethyl acetate require rather drastic conditions, i.e., prolonged heating of the adduct in vacuo. The characteristic host network in the adduct collapses upon guest removal, as shown by the change in the X-ray powder diffraction patterns. The resulting guest-free apohost, however, readily re-adsorbs the guest as a gas, liquid, or solid (Scheme 10), thereby restoring the original crystal structure of the adduct **21·2G**.[12c] This behavior is by no means a unique aspect of the present system but rather a common feature shared by many other cases of inclusion complexes. In Figure 1 is shown a typical "binding isotherm" for apohost **23** under fast-scanning conditions (○), where the guest is gaseous ethyl acetate. In the sorption process, sudden guest binding occurs at a threshold point ($P_{th} \cong 20$ Torr) and saturation (guest/host $\cong 2$) is reached at higher guest pressures. In the reverse direction with decreasing guest pressures, practically nothing happens and adduct **23·2G** survives beyond the threshold point. The sorption and desorption processes are far from reversible. In reality, however, the highly irreversible "binding isotherm" with a high degree of "hysteresis" is simply a kinetic consequence and hence apparent. A true or thermodynamic "binding isotherm" is obtained under slow-scanning

conditions (●), where sudden or vertical desorption takes place essentially at the threshold point for the desorption process.[19]

In 1998, we proposed that the present complexation (Scheme 10) should be treated as a phase equilibrium,[19] which should be governed by the phase rule, $f = c - p + 2$, where f is the degrees of freedom, c is the number of components, and p is the number of phases. Formation of calcium carbonate from calcium oxide and carbon dioxide (CaO + CO$_2$ → CaCO$_3$) is a textbook example of phase equiliblium. In this case, $c = 2$ (CaO and CO$_2$; CaCO$_3$ is not an independent component), $p = 3$ (solid CaO phase, solid CaCO$_3$ phase, and gaseous CO$_2$ phase), and hence $f = 2 - 3 + 2 = 1$. There is only one degree of freedom or variable in this equilibrium. If temperature as a sole variable is fixed at a certain value, the equilibrium pressure is also automatically fixed. In the present system, $c = 2$ (apohost **23** and guest; host–guest adduct is not an independent component) and $p = 3$ (solid apohost phase, solid adduct phase, and gaseous guest phase; note that adducts with different guests belong to different phases). Again, $f = 1$. Sharp sorption and desorption occurring at the threshold point, which is actually the equilibrium pressure, under the slow-scanning conditions (●) clearly indicates that the observed diagram is thermodynamic and is consistent with what the phase rule requires for a $2c/3p/1f$ system. At least from a thermodynamic viewpoint, it is not appropriate to use the term "binding isotherm." It should be referred to as a phase diagram.

Thus, there is no essential difference between the two reactions, i.e., formation of adduct **23·2G** and that of CaCO$_3$. As no one expects facile desorption of CO$_2$ from adduct CaCO$_3$ under ambient conditions, no one should expect facile desorption of included guest molecules from the adduct **23·2G**, either. The guest molecules are kinetically stabilized in the phase-changed adduct. If ready desorption of the guest, or the reaction product in the theme of the preceding section, is required, we need an $f = 2$ and hence $p = 2$ system free from guest-induced phase transition. This is the case where guest-free apohost and its complex share a common phase or in other words, where the guest binding cavity is maintained in the absence of a guest. We should move to robust metal-coordination networks. We did so but in an atypical manner as described in Section **3.6**. Before proceeding to that section, let me spend some more time on our continued effort on robust hydrogen-bonded networks.

3.5 Robust Hydrogen-Bonded Network. The guest-dependence of host **23** may essentially arise from the coordinative unsaturation of the hydrogen-bonded network (O–H···O–**H**) which achieves saturation only upon guest binding (O–H···O–**H**···O=C). If so, what about coordinatively saturated hydrogen bonds. A hint was anthracene–bis(pyrimidine) derivative **24**, which together with anthracene–bis(resor-
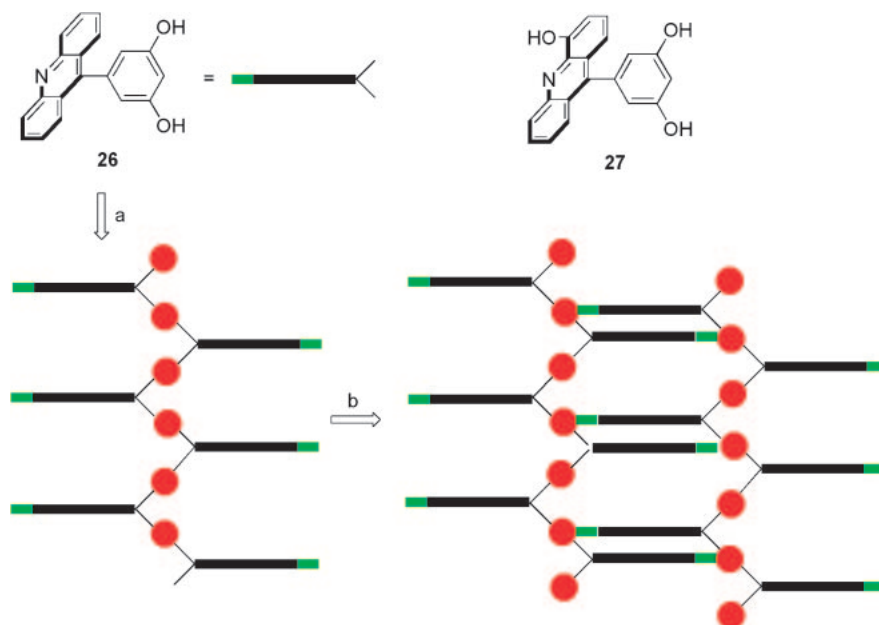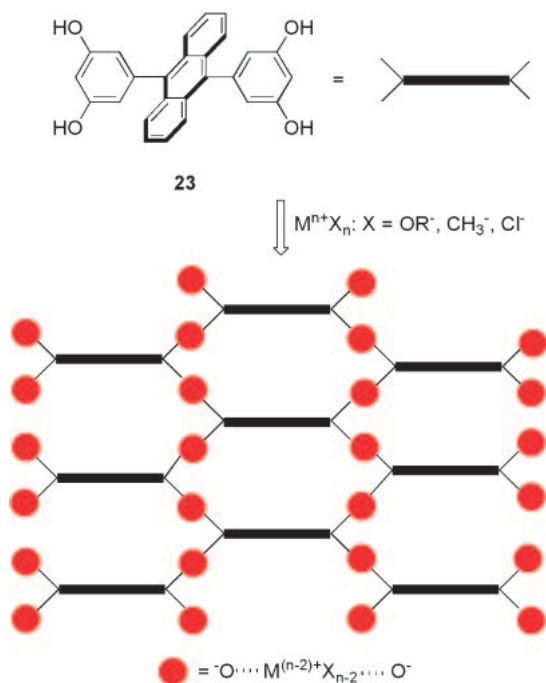
Scheme 11.

cinol) **23**, forms a guest-free 1:1 cocrystal **23·24** containing a saturated O–H···N network (Scheme 7). A model building block designed along this line is acridinylresorcinol **26**, which is self-complementary. When recrystallized from benzene, it affords a 1:1 complex **26**·benzene. In the crystal, host **26** forms a hydrogen-bonded (O–H···O–**H**) 1D chain (step a in Scheme 11) in a similar manner as the anthracene counterpart **25** (Scheme 8). In the acridine system, however, the chains come together via inter-chain O–H···O–**H**···N hydrogen bonding to form a coordinatively saturated 2D sheet containing cyclophane-like acridine stack dimers and cavities (step b), each of which incorporates two molecules of benzene.[20a] This network turns out to be considerably robust, since one of the two benzene molecules can be removed without inducing a phase change.

The robustness of the network can also be demonstrated in various ways.[20b] (1) Host **26** forms adducts with various polar and apolar guests. The stoichiometry or the number of guest molecules included in each cavity depends on their sizes; benzene and chloroform give rise to 1:1 adducts **26**·C_6H_6 and **26**·$CHCl_3$, while bulkier guests such as isobutyl benzoate and toluene afford 1:0.5 adduct **26**·0.5($C_6H_5CO_2C_4H_9$) and **26**·0.5($C_6H_5CH_3$). (2) The crystal structures, in terms of cell parameters and network- and cavity-defining distances and angles, of all the adducts including the half-desorbed benzene adduct **26**·0.5(C_6H_6) remain essentially the same, indicating that guest molecules adjust to the rigid cavity in this case, in marked contrast to the other (host **23**) case, where the flexible cavity adjusts to the guests. (3) The network is affected neither by the guest nor by a potentially hydrogen-bonding substituent on the host. Thus, hydroxyacridine derivative **27** (Scheme 11) behaves in the same manner as the parent host **26**, forming for example, adducts **27**·C_6H_6 and **27**·0.5($C_6H_5CH_3$) whose crystal structures are essentially the same as the parent adducts. Remarkably, the OH group in host **27** is not involved in any hydrogen-bonding interaction and is just staying as a spectator.

Clearly in the present case, the robust and rigid resorcinol–acridine O–H···N hydrogen-bonded network governs the crystal structure, and there is no room for the OH group on the acridine ring to participate. This is quite an exceptional case, since the potentially hydrogen-bonding OH group is usually a strong crystal-structure determinant. Introduction of an OH group often results in a drastic change in the crystal structures, as easily recognized when comparing the crystal structures of benzene and phenol.

3.6 Amorphous Organic Zeolite Catalysts. While apohost **23** as an insoluble organic solid showed a novel catalysis in the Diels–Alder reactions, its performance remained to be improved. In order to speed up intracavity reactions, one needs stronger activation of the dienophile which, in case of catalysis by **23**, is hydrogen-bonded (O–H···O–H···O=C) to the host network acting as a weak Brønsted acid. In order to speed up turnover of the catalyst, one needs, in light of discussion in Section **3.4**, permanent cavities free from product inhibition. A solution to both issues seemed to lie in the use of a robust metal-coordination network with Lewis acid as a metal center. We wanted to simply convert the hydrogen-bonded network (O–H···O–H) in host **23** (Scheme 6) to a metal-coordinated one ($^-$O···M^{n+}···O$^-$) by using a simple procedure which might be called an organic sol–gel process. It worked.

Treatment of host **23** with [Ti{Cl(O^{i}Pr}_2}], Al(CH_3)_3, or Zr(O^{t}Bu)_4 affords a highly insoluble, solvent-free 1:2 adduct **23**$^{4-}$·2[TiCl(O^{i}Pr)] (Ti host)[21], **23**$^{4-}$·2(AlCH_3) (Al host)[21], or **23**$^{4-}$·2[Zr(O^{t}Bu)_2] (Zr host)[22] as amorphous powders. These formulations coupled with other evidence suggest that deprotonated tetraanionic species of the host (**23**$^{4-}$) are networked via O–metal–O bridges, as illustrated in Scheme 12 where red circles represent $^-$O···[Ti^{IV}Cl(O^{i}Pr)]$^{2+}$···O$^-$, $^-$O···[Al^{III}-(CH_3)]$^{2+}$···O$^-$, or $^-$O···[Zr^{IV}(O^{t}Bu)_2]$^{2+}$···O$^-$, although the amorphous nature of the Ti, Al, and Zr hosts preclude any confirmation of their structures. A fascinating aspect of these materials is their microporosity. They are capable of facile

Scheme 12.

sorption/desorpotion of various types of guests with a Langmuir-type reversible binding isotherm; there is no indication of guest-induced phase change. Analysis of the reversible N_2 adsorption according to standard procedures reveals that the Zr host is indeed microporous, having a specific surface area of $\approx 200\,\mathrm{m^2\,g^{-1}}$, a pore size of $\approx 0.7\,\mathrm{nm}$, and a particle size of $\approx 0.7\,\mathrm{\mu m}$.

The Zr host, and the Ti and Al hosts as well, catalyze the Diels–Alder reaction of acrolein and 1,3-cyclohexadiene in a remarkable manner (Scheme 13a). As a solid metal–organic catalyst, the Zr host has a formula-based turnover rate constant of $40\,\mathrm{h^{-1}}$, which far exceeds those of its components, i.e., the soluble Lewis acid $Zr(O^tBu)_4$ ($0.1\,\mathrm{h^{-1}}$) and the hydrogen-bonded insoluble organic network **23** ($0.3\,\mathrm{h^{-1}}$). The reaction can also be conducted in a flow system with the insoluble Zr host packed in a glass column and a reactant mixture as a mobile phase to give pure Diels–Alder product without contamination with the Zr host in regard to both organic and metallic components. There is little doubt that the Zr host serves as a completely insoluble catalyst, and indeed it can be used repeatedly without notable deactivation.

Diels–Alder reactions of methyl vinyl ketone, methyl acrylate, ethyl acrylate, and *tert*-butyl acrylate are also catalyzed, where the catalytic performance of the Zr host may be evaluated by comparing the rates or the half-lives (τ_{hetero}) of the reactions with those (τ_{homo}) catalyzed by the corresponding homogeneous catalyst (soluble $Zr(O^tBu)_4$) on a mol Zr basis under otherwise identical conditions.[22] The preference factors ($r = \tau_{\mathrm{hetero}}/\tau_{\mathrm{homo}}$) for the heterogeneous catalysis over the homogeneous decrease sharply with increasing steric bulkiness of the dienophiles, $r = 210$, 80, 20, 4, and 0.9 for acrolein, methyl vinyl ketone, methyl acrylate, ethyl acrylate, and *tert*-butyl acrylate, respectively. There is essentially no catalysis by the Zr host for the bulkiest *tert*-butyl ester.

The observed trend in steric or bulkiness control of the reactions parallels with the binding (adsorption) selectivities of the present dienophiles toward the Zr host; competition between methyl acrylate and *tert*-butyl acrylate, for example, is in favor of the former with a selectivity factor of 98:2. These results leave little doubt that the reaction indeed takes place in the cavities (micropores) of the Zr host, where the included dienophile is coordinated with the metal center acting as a strong Lewis acid (Scheme 13a), as confirmed independently by IR measurements.

The Zr work, I hope, made an important step toward environmentally-friendly catalytic systems using organic or metallo-organic zeolite-type materials (organic zeolites) as insoluble, recoverable, and reusable catalysts with minimized waste. Speaking of wastes however, the use of organic solvents is not welcome. We want to use water as solvent. The present Zr network, and the Ti and Al networks as well, cannot survive under aqueous conditions. They readily undergo hydrolysis and collapse. After a number of trials, we reached a lanthanum system.[23] Treatment of apohost **23** with 2 equivalents of $La(O^iPr)_3$ in THF followed by aqueous workup affords an amorphous 1:2 adduct $\mathbf{23}^{4-}\cdot 2(\mathrm{LnOH})\cdot 6H_2O$ (La host) (Scheme 12 where red circles represent $^-O\cdots[Ln^{III}(OH)]^{2+}\cdots O^-$ and included water molecules are omitted for clarity). It is microporous in a similar manner as above. In marked contrast to the Zr case, the La host, which is completely insoluble in water, is stable in aqueous environments. When dipped in an aqueous solution of cyclohexanone, the La host picks up ≈ 6 molecules of the ketone, as a result of water/ketone exchange. In D_2O, the ketone undergoes facile H/D exchange at the α-positions of the carbonyl group; the kinetics of this reaction is consistent with a scheme (Scheme 13b) involving pre-equilibrium binding of the substrate ketone to the La host ($K = 5.8\,\mathrm{M^{-1}}$), followed by rate-determining enolization of the latter ($k = 0.01\,\mathrm{min^{-1}}$) conceivably via cooperation of the metal center as a Lewis acid and metal-coordinated OH^- (OD^-) as a Brønsted base. In the presence of benzaldehyde as an enolate acceptor, ketone–aldehyde cross-Aldol condensation takes place with the La host as a microporous enzyme (enolase) mimic.[24]

3.7 Leaving the Organic Zeolite Area.   While organic zeolite catalysts appeared to be potentially applicable to many other types of reactions, I actually left the field. This was partly because the CREST project on organic Zeolites was over. The more essential reason was that all the catalytically active, high-performance microporous solids we had dealt with were amorphous. At the same time, the completely amorphous nature of the catalysts led me to wonder if there was any reason why catalytically active microporous metallo-organic solids of the Lewis acid type should be amorphous.

Metal complexes require coordinative saturation. Catalytically active metal complexes should be coordinatively unsaturated at least dynamically so as to provide an open coordination site for the substrate. In homogeneous systems, solvent molecules come to play. Coordination of substrate may not be a big problem in view of facile ligand/solvent and solvent/substrate exchange. Such a process is hardly conceivable for complexes in the solid state. Thus, a question is how the present organic zeolite catalysts simultaneously fulfill
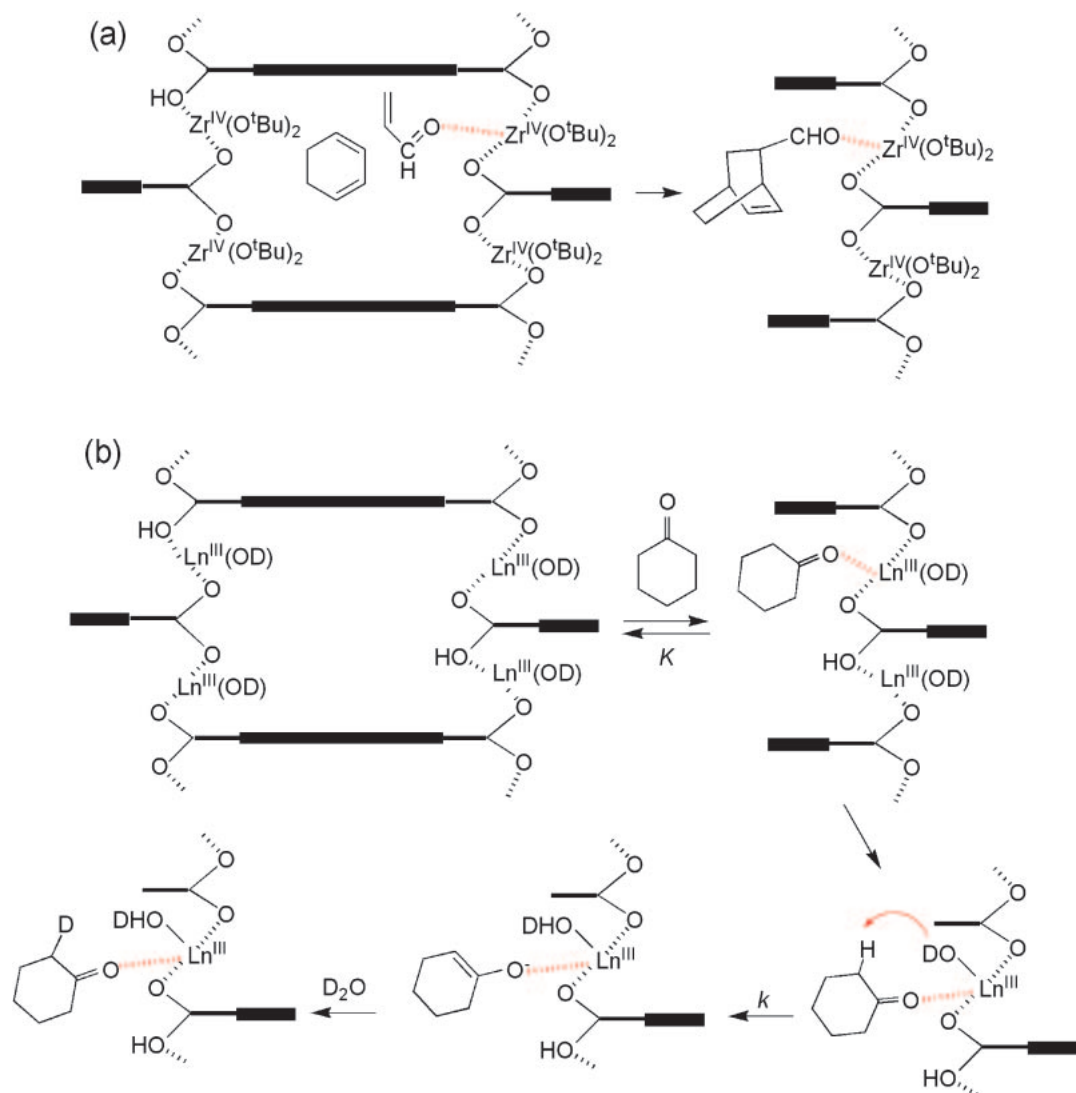
Scheme 13.

coordinative saturation in a structural sense and coordinative unsaturation in a kinetic (reactivity) sense.

An ^{27}Al solid MAS NMR study indicates that the catalytically active Al host $23^{4-}\cdot2(\text{AlCl})$, obtained by treatment of apohost **23** with $\text{Al}(CH_3)_2Cl$, possesses both saturated (hexacoordinated) and unsaturated (tetracoordinated) Al centers.[25] Thus, the structure is not so simple as the formula suggests in reference to Scheme 12 where in the present case, red circles represent $^-\text{O}\cdots[\text{Al}^{\text{III}}(\text{Cl})]^{2+}\cdots\text{O}^-$ and hence the Al^{III} centers are formulated as tricoordinated). As in simple metal alkoxide $(\text{Al}(\text{O}^i\text{Pr})_3)$, the metal centers must be bridged by the ligands but not extensively, plausibly by the steric constrain of the host network. The unsaturated (tetracoordinated) metal centers might be stabilized via dynamic delocalization with the saturated (hexacoordinated) centers in a similar manner as borane (BH_3) can be stabilized in a formal valency of 3.5 in the form of diborane (B_2H_6) with bridging hydrogen (H) ligands. This might explain why the catalytically active, porous metallo-organic solids (organic zeolites) should be amorphous. This hypothesis, however, was far beyond my ability to prove.

4. Huge but Finite Nano Systems Based on Hydrogen Bonding in Water

4.1 Paradigm Shift from Sugars as a Guest to Sugars as a Probe. Oligosaccharides on cell surfaces play important roles in various cellular communication events. We naturally got interested in sugar binding in water. Sugars however, are tough guests in water. They are highly hydrophilic, and characteristic sugar OH groups are not easily accessible. This is because relevant hydrogen-bonding interactions do not work effectively in water, which itself is potentially hydrogen bonding. We first paid attention to the CH–π interactions between polarized C–H bonds (HO–C–H) of the sugar and an electron-rich aromatic π base of a host. It worked but modestly at best.[26–28] Instead of escaping at that point, we had to face hydrogen bonding in water.

Cell-surface oligosaccharides usually occur as clusters and their interactions with lectins (sugar binding proteins) are often claimed to be multivalent. The advantage of such a multiple interaction is referred to as the cluster or multivalency effect, and is relevant to the generalization we made before
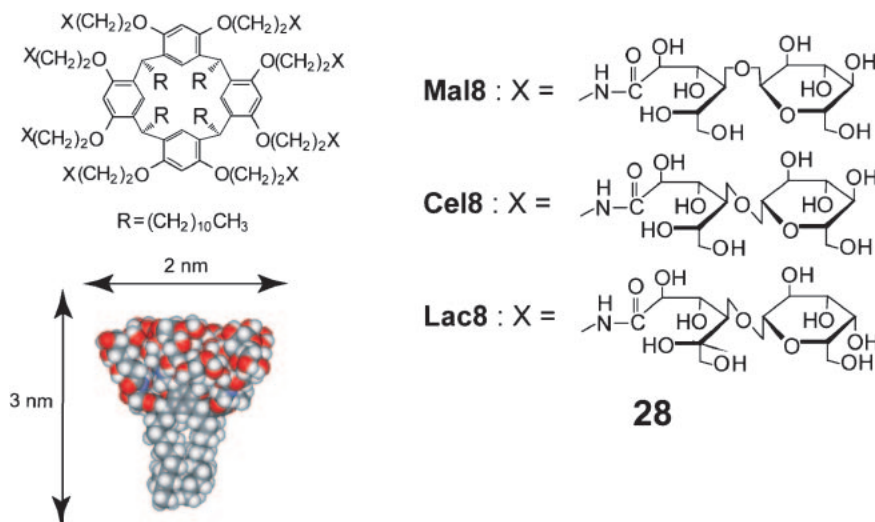
Chart 6. Structures **28**.

(Section **2.4**). We paid much attention to clustering sugar moieties as a guest but, as readily anticipated, it was not an easy task to design appropriate hosts without enough knowledge of the polar interactions in water. Probably, a more relevant question would be how such a sugar cluster behaves in water. Since sugars are highly hydrophilic and usually uncharged, they are least susceptible to major complexation-driving forces in water, i.e., hydrophobic effects and electrostatic attractions aided thereby. Thus, the association behavior of a sugar cluster in water must reflect hydrogen-bonding or, more generally, polar interactions. This was an important paradigm shift for me from sugars as a guest to be captured to sugars as a probe to tell us about polar interactions in water.

4.2 Macrocyclic Glycoclusters and Their Adhesive Nature. We took advantage of the calix[4]resorcarene framework on which to assemble sugar moieties. Octaol **17c** (Section **2.3**) having four long (undecyl) chains was converted to the octakis(2-aminoethoxy) derivative (OH → OCH$_2$-CO$_2$Et → O(CH$_2$)$_2$OH → O(CH$_2$)$_2$NH$_2$), which readily reacted with lactone derivatives of disaccharides (higher oligosaccharides as well) to result in fixation of the latter on the macrocyclic skeleton via ring-opened amide linkages. Thus, maltonolactone, cellobiolactone, and lactonolactone give rise to octa(glycoside) compounds **28** (Chart 6) with non-reducing terminal sugar moieties in the intact pyranose form, i.e., *α*-glucoside (Mal8), *β*-glucoside (Cel8), and *β*-galactoside (Lac8), respectively. The resulting glycocluster compounds (Mal8, Cel8, and Lac8; molecular weight, 4172) having a definite number (eight) of saccharide moieties in a well-defined geometry may represent a unimolecular motif of saccharide clusters on the cell surface. The four long alkyl chains, originally introduced to enhance lipophilicity (Section **2.3**), turn out to play an important role in aggregation of the molecular glycocluster into glycocluster nanoparticles, as shown later.

Glycocluster **28** is highly hydrophilic. It is miscible with water and is hardly soluble even in methanol. Nevertheless, it is highly adhesive in water and is readily adsorbed on polar solid surfaces such as quartz (silica) conceivably via polar (hydrogen bonding) interactions between sugar OH groups and quartz silanol (SiOH) moieties.[29] Glycocluster **28** is also easily bound to lectin (sugar binding protein) in a specific manner.[30] Thus, glucose-cluster compound Mal8 is bound to glucose/mannose binding concanavalin A but not to galactose binding peanut lectin. Galactose-cluster compound Lac8, on the other hand, is picked up by peanut lectin but not by concanavalin A. Lac8 but not Mal8 can also be bound to hepatic cells having an asialoglycoprotein receptors for the terminal galactose residues.[31] The saccharide selectivity is remarkably high and there is no crossover. As a calix[4]resorcarene derivative, the present glycocluster compounds possess a vase-shaped aromatic cavity in which a hydrophobic guest, dye stuffs in particular, can be easily incorporated.[32] The adsorption of glycocluster **28** on the polar solid surfaces and sugar binding sites of receptor proteins (lectins and asialoglycoprotein receptors) occurs not only as such (guest-free apohost) but also as its guest adduct. In this context, the glycocluster host acts as a transporter to deliver guest molecules to the solid surfaces and protein sites.[29–31] From a structural point of view, however, there was an annoying problem. If glycocluster **28** is adsorbed on the quartz surface in a face-to-face fashion, the four long alkyl chains must be exposed to bulk water. Energetically, this is highly unfavorable. Interaction of artificial substrates with a receptor protein is often accompanied by nonspecific binding arising mostly from the hydrophobic nature of the former. In these regards, how can the presence of long, hydrophobic chains in the present glycocluster compounds be compatible with the observed binding mode and binding specificities?

Judging from its structure, glycocluster **28** is expected to form micelle-like aggregates in water. Actually however, it is not surface-active. This dilemma was solved from a combined GPC and TEM study.[33] It indeed forms micelle-like spherical aggregates with a diameter of 4–5 nm and an aggregation number of ≈6 (Scheme 14, step a). In marked contrast to usual cases, the present "micellization" is practically irreversible. There is no equilibrium dissociation of the "micelle" into monomers. As a consequence, there is no equilibrium distribution of monomers at the water–air interface and hence no surface activity, either. Strong intermolecular hydrophobic
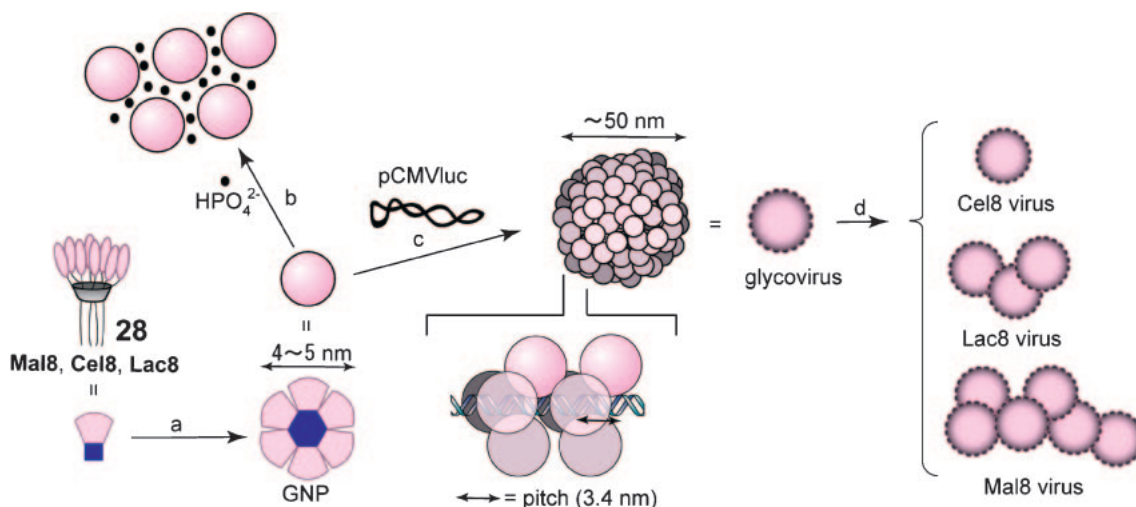
Scheme 14.

entangling of the alkyl groups in quadruple-chain amphiphile **28**, coupled with possible lateral or intercluster hydrogen bonding in the glycocluster layer, may make the present micelle (hereafter called glycocluster nanoparticle (GNP)) unusually stable. The hydrophobic alkyl chains of glycocluster amphiphile **28** are thus effectively masked upon irreversible formation of GNP. The glycocluster compound **28** as GNP with masked hydrophobicity can thus be effectively adsorbed on the quartz surface and bound to right proteins in a highly saccharide-specific manner.

4.3 Marriage of Sugar and Salt via Hydrogen Bonding.
The polar interaction of the glycocluster in water was highlighted in its unexpected affinity to the phosphate ion.[33,34] This was quite serendipitous. When a solution of glycocluster **28** (Mal8) in aqueous phosphate buffer is left for a long time, turbidity occurs. This is more pronounced, with formation of precipitates, for glycoclusters having longer oligosaccharide chains derived for example, from higher homologs of maltose, such as maltopentaose, -hexaose, and heptaose. The precipitates consist of both organic (glycocluster) and inorganic (sodium phosphate) components. A combined NMR, DLS, AFM, TEM, and calorimetric study of a solution of Mal8 (0.1 mM) and Na_2HPO_4 (10 mM) reveals the nature of the interaction between them. (1) DLS shows that the particles present in the solution grow in size from several nm for GNP (glycocluster nanoparticle) to ≈ 70 nm. (2) AFM and TEM confirm the formation of particles in this size range; the particles being actually composed of smaller GNPs. (3) ^{31}P NMR titration indicates that the chemical shift of the phosphate dianion undergoes an Mal8-induced upfield shift with a well-behaved binding isotherm with $K_{app} = 7 \times 10^3\,M^{-1}$ for a unit binding site. The upfield shift indicates that the phosphate dianion undergoes partial protonation. (4) Isothermal titration microcalorimetry reveals that the present glycocluster–Na_2HPO_4 complexation is driven by a favorable entropy change with $\Delta H^0 = 11.2\,kJ\,mol^{-1}$, $\Delta S^0 = +111\,J\,mol^{-1}\,K^{-1}$, and $K_{app} = 8.5 \times 10^3\,M^{-1}$ which is in fairly good agreement with $K_{app} = 7 \times 10^3\,M^{-1}$ obtained from NMR.

All the observations presented above suggest that GNPs undergo agglutination with the phosphate ions as a glue

(microscopic evidence) (Scheme 14, step b). The glycocluster–phosphate interaction must be polar, of a sugar-to-phosphate $O–H\cdots^-O–P$ hydrogen-bonding type (NMR evidence), since the glycocluster is neutral and has no charge and its partner, the phosphate ion, has no element of hydrophobicity and there is no room, at least in the formal sense of the words, for the hydrophobic and electrostatic interactions to come to play in the present complexation. Agglutination of GNPs can also be induced by other anions such as sulfate and perchlorate. The formation of GNP network mediated by the multivalent anions may further induce inter-particle, i.e., inter-GNP, sugar–sugar hydrogen bonding. This may result in desolvation (dehydration) of GNPs, i.e., liberation of many water molecules bound on the highly hydrophilic GNP particles and phosphate anions, in accord with the thermodynamic aspect of the present complexation which is entropy driven. Sugar and salt are two representative classes of highly hydrophilic or water-soluble substances. In the present system, they (glycocluster and sodium phosphate) escape from the otherwise comfortable hydration shells to get married.

4.4 Glycoviruses from Size-Coated Gene Coating with Glycocluster Nanoparticles (GNP). The GNP–phosphate interaction led us to take up DNA, a natural phosphate polymer, as an interaction partner of GNP.[35] We use plasmid DNAs, which are small cyclic DNAs often used to deliver particular genes into the cell. An example is pCMVluc which consists of 7040 bp (bp = base pairs), containing a cytomegalovirus promoter followed by the gene encoding firefly protein luciferase. The complexation with pCMVluc of cellobiose-derived glycocluster (Cel8) (Scheme 14, step c) is readily monitored by gel electrophoresis. With increasing Cel8/DNA or Cel8/N ratios (N represents the nucleotide unit of DNA), pCMVluc is rendered completely immobile at Cel8/N $\cong 0.6$. DLS, on the other hand, reveals that huge aggregates occur at lower Cel8/Ns but they become smaller at higher Cel8/N's until saturation is reached at Cel8/N $\cong 0.6$ with a saturation DLS size of $d_{DLS} \cong 50$ nm. The TEM image of the particle (hereafter called glycovirus) is virus-like, being composed of compactly packed, several-nm sized GNPs (Figure 2a; letter N means negative staining). The stoichiometry of Cel8/N = 0.6,
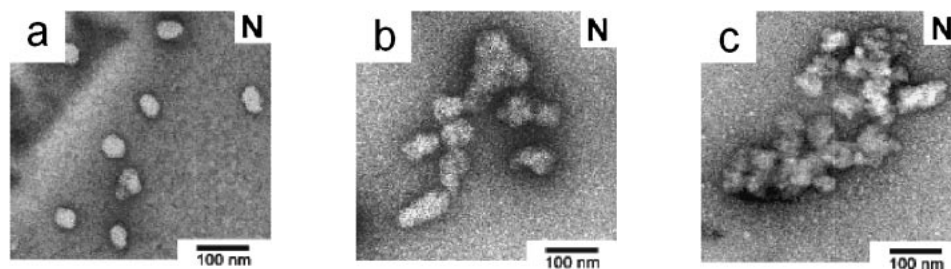
Figure 2. TEM (transmission electron microscopic) images of the Cel8 (a), Lac8 (b), and Mal8 (c) viruses under negative (N) staining (uranyl acetate) conditions.

i.e., Cel8:N = 0.6:1 = 12:20, indicates that two particles of GNP composed of six molecules of glycocluster Cel8 are accommodated in every helical pitch of the DNA composed of 10 bp. The helical pitch of B-type DNAs is 3.4 nm, which is shorter than the size (4–5 nm) of GNP. Two GNP particles, presumably accommodated in the major and minor grooves in every pitch, may be arranged either north–south or east–west alternately pitch by pitch to avoid GNP–GNP steric interference, as illustrated in Scheme 14. Glycoclusters Lac8 and Mal8 complex pCMVluc in a similar manner to give Lac8 and Mal8 viruses. In marked contrast to the Cel8 virus, they undergo further aggregation (Scheme 14, step d) as confirmed by TEM (Figures 2b and 2c, respectively) and DLS with average sizes of $d_{DLS} = \approx 200$ and ≈ 300 nm for Lac8 virus and Mal8 virus, respectively. The monomeric Cel8 virus, moderately aggregated Lac8 virus, and more extensively aggregated Mal8 virus turn out later to serve as a unique set of probes to reveal the size effect in gene delivery (vide infra).

From a structural viewpoint, viruses contain a single genetic molecule (DNA or RNA) covered with closely packed protein molecules with a strict stoichiometry. The present glycoviruses share with real viruses such characteristic features as unimolecularity with respect to DNA, stoichiometry, although not strict, close packing, and characteristic appearance reflecting thereof. From a functional view point, viruses transfect cells, i.e., enter the cells and make the genetic information coded in viral DNA or RNA expressed into proteins. If the present glycoviruses can be so called, they must be transfectious. This is indeed the case.[35] The present glycocluster compounds, particularly cellobiose-derived (Cel8), are capable of delivery of pCMVluc into cultured cells such as HeLa, a malignant uterine cell line, and HepG2, a malignant hepatic (liver) cell line, as confirmed by chemiluminescence assay of the firefly protein luciferase expressed in the cells. This itself is rather surprising, since to the best of our knowledge there is no precedent of neutral species acting as an effective gene carrier. In numerous studies on artificial or nonviral gene delivery, cationic polymers and cationic liposomes have been extensively used as gene carriers. This is not simply because they readily form complexes with polyanionic DNAs but also because the resulting carrier–DNA complexes with a net positive charge can be easily adsorbed on the cell surface which is negatively charged in general. The present glycoviruses are neutral and there can be no electrostatic assistance. The neutral glycoviral gene delivery is actually size-promoted.[36]

4.5 Size-Controlled Glycoviral Gene Delivery. In Figure 3 are shown the transfection efficiencies evaluated by
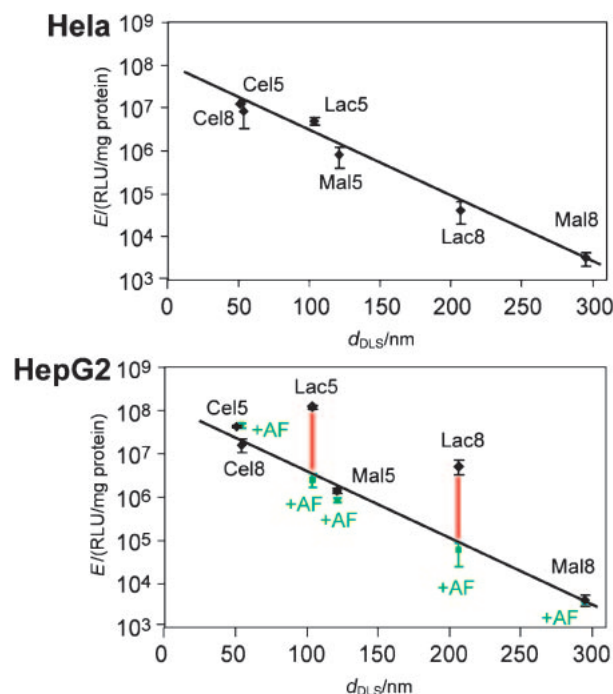
Figure 3. Glycovirus-mediated transfection of HeLa cells and HepG2 cells. Luciferase expression efficiencies in terms of chemiluminescence relative light units (RLU) per mg total protein as a function of the size of glycoviruses. Those with a mark +AF refer to the runs in the presence of asialofetuin as an inhibitor.

chemiluminescence assay (RLU = relative light unit per mg protein), plotted against DLS sizes of various glycoviruses derived from fully saccharide-functionalized glycoclusters Cel8, Lac8, and Mal8 as well as partially (on five (on average) amino groups out of eight) saccharide-functionalized Cel5, Lac5, and Mal5.[36] Zeta potential measurements show that all the glycoviruses investigated have neutral (≈ 0 mV) surfaces, indicating that the positive charge if any arising from the free ammonium groups in the Cel5, Lac5, and Mal5 viruses is effectively masked by saccharide coverage. In the case of HeLa cells, the transfection efficiencies sharply decrease with increasing sizes of the glycoviruses. Only monomeric Cel8 and Cel5 viruses are practically active. A similar size-activity correlation is found also in the case of HepG2 cells which, as a hepatic cell line, possess asialoglycoprotein receptors for the terminal galactose residues. Indeed, the Lac8 and Lac5 viruses have a much higher activity than expected from the size
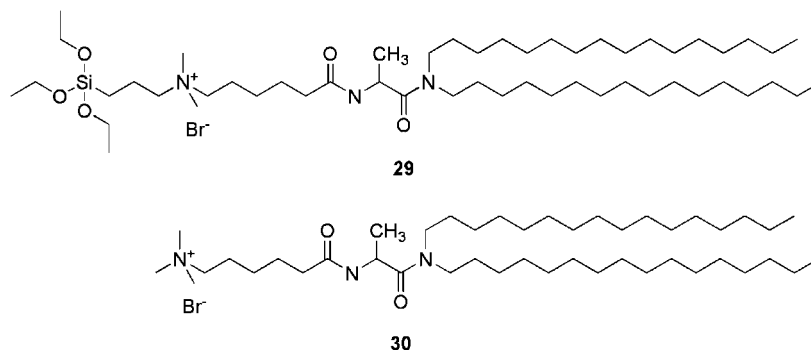
Chart 7. Structures **29** and **30**.

correlation. This extra activity (shown in red bars) arises from the specific receptor pathway involving the galactose receptors on the cell surface and the terminal galactose residues in the Lac viruses, as confirmed by inhibition study using asialofetuin as a blocker of the receptor site (Figure 3). Unfortunately, however, this receptor advantage for the Lac viruses is canceled by the size factor, i.e., by the aggregating nature of the Lac viruses. A further systematic Lac-functionalization study indicates that the size and receptor factors are optimized at Lac3 virus, derived from glycocluster having ≈3 lactose moieties, which is monomeric, neutral, and hepatocyte-targeting.[37]

Endocytosis is the drinking activity of eukaryotic cells, by which external substances are swallowed in the cell and accommodated in the endocytic vesicles having a size of ≈100 nm. The observed size effect in glycoviral gene delivery may be understood in this context; monomeric Cel viruses of ≈50 nm can be taken into the vesicles, while even dimeric or trimeric Lac viruses (≈200 nm) and more extensively aggregated Mal viruses (≈300 nm) may be hardly accommodable. With the highest activity of the Cel viruses being understood in this way, what about the size effect in the subviral (≪50 nm) region? A competitive experiment using glycocluster nanoparticle (GNP) ($d \cong 5$ nm), Mal8-coated CdSe quantum dot ($d \cong 15$ nm), and monomeric Cel8 virus ($d \cong 50$ nm), which have similar saccharide-coated surface structures and are otherwise closely related to each other, shows that cellular uptake activities decrease in the order monomeric virus > quantum dot > GNP.[38] Thus, the endocytic cellular uptake is optimized at the viral size (≈50 nm). This may be understood in terms of size complementarity between the endocytic vesicle as a giant host and the (glycol)virus as a giant guest.

4.6 Cerasome as a Cationic Gene Carrier with a Viral Size.   As referred to above, cationic liposomes and polymers have been extensively used as nonviral gene carriers. They endow the resulting carrier–DNA complexes a net positive charge, which is supposed to be essential for the complexes to be adsorbed on the negatively charged cell surface. The above results for the Cel viruses clearly indicate that this is not necessarily true. If size is appropriate, there is no need of electrostatic assistance. Cationic gene carriers, on the other hand, generally have a problem in size control. For example, cationic liposomes easily undergo fusion when bound to DNA.

In collaboration with the group led by J. Kikuchi, we proposed the cerasome strategy for infusible liposomes.
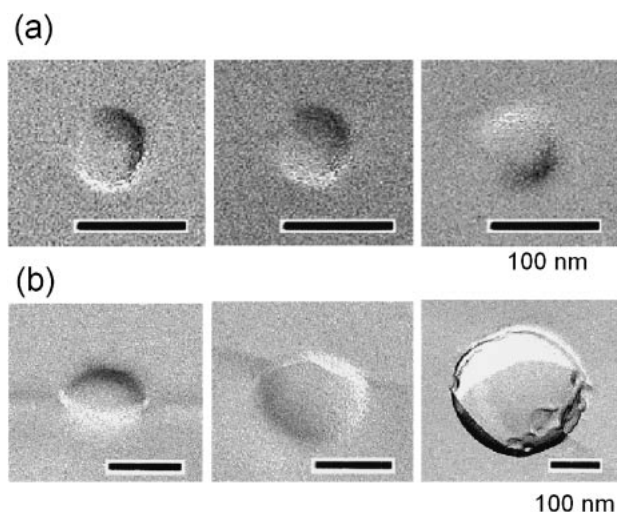
Figure 4.   Freeze-fracture TEM images of the **29**–plasmid (a) and **30**–plasmid (b) complexes. Approximately ten images were taken for each samples and three of them, including the smallest one and the largest one, are shown.

Sonication of an aqueous dispersion of triethoxysilylated peptidic lipid **29** (Chart 7) affords bilayers with a concomitant sol–gel process (EtO–Si– + H₂O → Et–OH + –Si–OH, 2(–Si–OH) → –Si–O–Si– + H₂O) on the surface to result in the formation of silica- or ceramic-coated liposomes (cerasomes)[39] in a viral size (60–70 nm). The surface-rigidified cerasomes turn out to be infusible upon complexation with a luciferase-coding plasmid DNA, retaining the original viral size (≈70 nm) (Figure 4a).[40] Nonsilylated reference lipid **30** also affords liposomes in a similar size. In marked contrast to cerasomes, however, the reference liposomes undergo fusion upon complexation with the plasmid to give bigger particles (100–300 nm; mostly ≥200 nm) (Figure 4b). The size effect in transfection is dramatic. The transfection efficiency of the infusible cerasome-forming lipid **29** is higher than that of the fusible liposome-forming reference lipid **30** by a factor of 10^{2-3}.[40,41]

The transfection efficiency is governed by many factors such as charge, size, and the presence/absence of a targeting ligand. They are closely related to each other. For example, introduction of a galactose residue to a cationic carrier for hepatocyte targeting would likely change the surface charge of the carrier–DNA complex. The change in charge would possibly change the size as well. This interdependence makes it very difficult to

carry out systematic structure–activity correlation studies. A real problem in artificial gene delivery lies in this very point. Our approach probably provides the first successful case in this regard.[35,36] By using neutral glycoviruses as size markers, we first demonstrate unambiguously the size effect in gene delivery. On the observed size-activity correlation, we then substantiate the contribution of the receptor pathway for Lac viruses targeting the hepatic HepG2 cells. Now, we reach infusible cerasomes free from size depression. Interestingly, the size factor of 10^{2-3} (vide supra) arising from a size difference between monomeric **29**–plasmic complex ($\approx$70 nm) and fused **30**–plasmid complex ($\geq$200 nm) is in fairly good agreement with that expected on the size-activity correlation (Figure 3) established for the neutral glycoviral gene delivery.

5. Manipulated Biological Systems with Functional In-Cell Devices

5.1 Molecular Beacon-Type Riboregulator for Gene Sensing. With high-performance gene-delivery systems in hand, we wanted to step further into the biological field. It would be most interesting to open an important yet unexplored area of biological significance using chemical tools. An area which attracted us is in-cell monitoring of genetic materials. Along this line, we started a new program on gene sensing with its potential in-cell application.

Gene sensing relies on target-probe hybridization, based on G–C and A–T (DNA) or A–U (RNA) base-pairing, coupled with a report tool. Molecular beacon is a typical sensing probe. It consists of three parts, a target binding domain, a couple of self-complementary sequences outside the target binding domain, and a fluorophore and quencher pair located at the termini. In the absence of target, it forms a hairpin structure with a stem region consisting of base-paired self-complementary sequences. The fluorophore and the quencher are forced in proximity, the former being rendered nonfluorescent as a result of efficient FRET (fluorescence resonance energy transfer). In the presence of target, target-probe hybridization opens the hairpin structure to free the fluorophore from FRET; the former now emits fluorescence, i.e., target-induced fluorescence. While cleverly designed, molecular beacon probes with no signal amplification mechanism and with possible cytotoxicity are hardly applicable to in-cell gene sensing. Its efficient delivery to the cells can itself be a problem. Our strategy is to couple the molecular beacon-type on/off regulation to biological protein translation to allow target-induced production of a chemiluminescent protein instead of target-induced light-up of a FRET pair.

The designed, molecular beacon-type mRNA probe is composed of four parts, an ORF (open reading frame with a start codon AUG) for chemiluminescent firefly luciferase as a reporter protein, a ribosome binding sequence (RBS) shown in red, a target binding site (probe) shown in yellow, and an antiRBS or RBS-docking sequence which is complementary to RBS (Scheme 15). In the absence of target, the probe forms a hairpin with RBS–antiRBS base-pairing forming a stem. The RBS, whose binding capacity is used toward antiRBS, is not accessible to the ribosome which is the essential translation machinery. The whole system is translation-off as a result. In the presence of target (shown in black in Scheme 15), the

Scheme 15.

hairpin structure is opened upon target-probe hybridization with the concomitant result of liberation of RBS from antiRBS. The ribosome now binds to freed RBS to start translation of the reporter protein luciferase, whose chemiluminescence, i.e., target-induced chemiluminescence can be easily monitored by standard chemiluminescence assay.
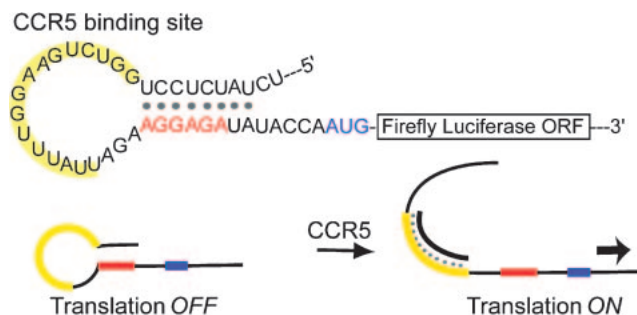
The present molecular beacon-type mRNA (riboregulator) probes can indeed sense the 16-mer (620–635) oligonucleotide sequence of human chemokine receptor 5 (CCR5) in an in vitro translation system at a fmol level with single-nucleotide resolution.[42,43] There are a number of attractive aspects in the present system. (1) The present mRNA probe with no functionalization with organic dye can be applied also in the form of double-strand DNA, which is in situ transcribed into RNA in an in vitro translation system or in live cells, (2) the present system is signal-amplifying, since the transcription (DNA to RNA), translation (RNA to protein luciferase), and the chemiluminescence-generating, enzymatic sensing reaction of luciferase are all catalytic, and (3) the choice of reporter proteins in terms of wavelength or color of chemiluminescence is arbitrary so that one can assign different colors to different alleles of the target to allow multicolor sensing of SNP (single nucleotide polymorphism).[44]

5.2 Light-Up Aptamer–Fluorophore Pair for Transcription Monitoring. The Nobel Prize in Chemistry for 2008 went to the discovery of green fluorescent protein (GFP) and its application. The application of GFP was in the fusion technology thereof. Proteins of interest can be fused to GFP and afford upon transcription/translation fusion proteins with GFP. The target proteins can be monitored with GFP as a fluorescent tag. What we wanted to do was in-cell monitoring of RNAs. In analogy with the GFP-fusion technology, we need a fluorescent RNA tag. Unfortunately however, fluorescent RNAs are not known. In these circumstances, we set up a two-step evolution strategy for "light-up" RNA–fluorophore pairs as a tag.

The first step is chemical evolution of dyestuffs. Hoechst 33258 (**31**) (Chart 8) is a microenvironment-sensitive fluorophore whose fluorescence intensity is highly dependent on the micropolarity of the environment. It is practically nonfluorescent in water but is rendered highly fluorescent when bound to the minor groove of double-strand (ds) DNAs. As a consequence, it is used as a stainer of nucleus in live cells. The Hoechst dye possesses a number of attractive features (light-up upon binding to nucleic acid, cell permeability, and low cytotoxicity) as an RNA imager. The problem is its high

Y. Aoyama

Bull. Chem. Soc. Jpn. Vol. 82, No. 4 (2009)   437

Chart 8. Structures 31–33.

affinity to dsDNA. Our target is RNA in the cells. We thought that the affinity to dsDNA could be sterically controlled. In fact, upon introduction of two bulky *ter*t-butyl groups on the benzene ring, the dye loses its affinity to dsDNA.

The second step is biological evolution of random RNA sequences into particular ones that specifically bind to a *ter*t-butyl-modified or "evolved" dye by using the in vitro selection (or in-test tube evolution) scheme known as SELEX (systematic evolution of ligands with exponential enrichment). It is composed of two essential processes, selection of random sequences on the target by using in the present case, target-immobilized magnetic particles and PCR (polymerase chain reaction) amplification of the binding sequences (aptamers). By repeating the selection/amplification cycles, one can exponentially enrich or evolve the strongly binding aptamers with K in the order of 10^6 and $10^8 \, M^{-1}$ for the DNA[45] and RNA[46] aptamers, respectively. Partial sequences of the aptamers, in light of their computer-predicted secondary structures, were also checked in search for the true dye binding domain of the aptamers. In this way, we reached the shortest optimized (in terms of light-up property) sequences, i.e., 25-mer DNA aptamer **32** with $I/I_0 = 190$[45] and 29-mer RNA aptamer **33** with $I/I_0 \geq 50$,[46] where I_0 and I are fluorescence intensities of the modified dye when alone and when bound to the optimized aptamer, respectively. The aptamer–fluorophore (29-mer RNA aptamer-modified dye) pair can be used as a fluorescence tag. Transcription of luciferase gene fused with five successive 29-mer RNA tag sequences in an in vitro transcription system can indeed be fluorescence-monitored in the presence of the modified dye.[46]

6. What Did I Want to Know? A Closing Remark

It has been 35 years since I started my academic carrier as a research associate at Kyushu University in 1974. Reviewing here the main stream of my research, I have mixed feelings. It is evident that the whole work is more or less design-based. To be honest, I have satisfaction with what we could have done or what we could have designed. Design, on the other hand, is based on what is known and as such it is limited. There are many unknowns and there could have been an unknown-based or curiosity-oriented approach. If the design-based approach is to lead to invention, the curiosity-oriented one would lead to discovery. The question to myself is: what really did I want to know and what did I discover in the last 35 years? Science and technology are closely related with each other as the two faces of a coin. This is especially true for chemistry and biology. The

design-based approach is bottom-up starting from sound knowns. Current nanotechnology and bionanotechnology are along this line. I have no objection to that. At the same time however, I strongly feel that we should never abandon a top-down approach starting from mysterious unknowns for the creation of new science. So, a question to dear young readers of this account: what do you want to know? What is mysterious to you?

It is my great honor to have been given this chance to review my research in the form of an Award Account. It is also my great pleasure to take this opportunity to express my deepest thanks to all of my former and present co-workers with whom I shared research days with at Kyushu University, Nagaoka University of Technology, and Kyoto University, my supervisor professors for their kind guidance, and my colleagues for their valuable collaboration and encouragement. Financial support from the Ministry of Education, Culture, Sports, Science and Technology, the Japan Science and Technology Agency (JST), Japan Society for the Promotion of Science (JSPA), and other funding agencies is also greatly acknowledged.

References

1 Y. Murakami, Y. Aoyama, K. Dobashi, *J. Chem. Soc., Perkin Trans. 2* **1977**, 24.

2 Y. Aoyama, T. Yoshida, K. Sakurai, H. Ogoshi, *Organometallics* **1986**, *5*, 168.

3 Y. Aoyama, A. Yamagishi, Y. Tanaka, H. Toi, H. Ogoshi, *J. Am. Chem. Soc.* **1987**, *109*, 4735.

4 a) Y. Aoyama, A. Yamagishi, M. Asagawa, H. Toi, H. Ogoshi, *J. Am. Chem. Soc.* **1988**, *110*, 4076. b) Y. Aoyama, M. Asakawa, A. Yamagishi, H. Toi, H. Ogoshi, *J. Am. Chem. Soc.* **1990**, *112*, 3145.

5 Y. Aoyama, M. Asakawa, Y. Matsui, H. Ogoshi, *J. Am. Chem. Soc.* **1991**, *113*, 6233.

6 a) Y. Aoyama, Y. Tanaka, H. Toi, H. Ogoshi, *J. Am. Chem. Soc.* **1988**, *110*, 634. b) Y. Aoyama, Y. Tanaka, S. Sugahara, *J. Am. Chem. Soc.* **1989**, *111*, 5397. c) K. Kurihara, K. Ohto, Y. Tanaka, Y. Aoyama, T. Kunitake, *J. Am. Chem. Soc.* **1991**, *113*, 444.

7 Y. Kikuchi, K. Kobayashi, Y. Aoyama, *J. Am. Chem. Soc.* **1992**, *114*, 1351.

8 Y. Tanaka, Y. Kato, Y. Aoyama, *J. Am. Chem. Soc.* **1990**, *112*, 2807.

9 Y. Kikuchi, Y. Kato, Y. Tanaka, H. Toi, Y. Aoyama, *J. Am. Chem. Soc.* **1991**, *113*, 1349.

10 Y. Kikuchi, Y. Tanaka, S. Sutarto, K. Kobayashi, H. Toi, Y. Aoyama, *J. Am. Chem. Soc.* **1992**, *114*, 10302.

11 Y. Tanaka, Y. Aoyama, *Bull. Chem. Soc. Jpn.* **1990**, *63*, 3343.

12 a) K. Kobayashi, K. Endo, Y. Aoyama, H. Masuda, *Tetrahedron Lett.* **1993**, *34*, 7929. b) Y. Aoyama, K. Endo, K. Kobayashi, H. Masuda, *Supramol. Chem.* **1994**, *4*, 229. c) K. Endo, T. Sawaki, M. Koyanagi, K. Kobayashi, H. Masuda, Y. Aoyama, *J. Am. Chem. Soc.* **1995**, *117*, 8341.

13 Y. Aoyama, K. Endo, T. Anzai, Y. Yamaguchi, T. Sawaki, K. Kobayashi, N. Kanehisa, H. Hashimoto, Y. Kai, H. Masuda, *J. Am. Chem. Soc.* **1996**, *118*, 5562.

14 K. Endo, T. Ezuhara, M. Koyanagi, H. Masuda, Y. Aoyama, *J. Am. Chem. Soc.* **1997**, *119*, 499.

15   For the molecular-alignment and guest-binding properties of porphyrin–bis(resorcinol) and porphyrin–mono(resorcinol) derivatives, see: a) K. Kobayashi, M. Koyanagi, K. Endo, H. Masuda, Y. Aoyama, *Chem.—Eur. J.* **1998**, *4*, 417. b) T. Tanaka, K. Endo, Y. Aoyama, *Bull. Chem. Soc. Jpn.* **2001**, *74*, 907.

16   K. Endo, T. Koike, T. Sawaki, O. Hayashida, H. Masuda, Y. Aoyama, *J. Am. Chem. Soc.* **1997**, *119*, 4117.

17   T. Dewa, T. Saiki, Y. Imai, K. Endo, Y. Aoyama, *Bull. Chem. Soc. Jpn.* **2000**, *73*, 2123.

18   T. Sawaki, K. Endo, K. Kobayashi, O. Hayashida, Y. Aoyama, *Bull. Chem. Soc. Jpn.* **1997**, *70*, 3075.

19   T. Dewa, K. Endo, Y. Aoyama, *J. Am. Chem. Soc.* **1998**, *120*, 8933.

20   a) T. Tanaka, K. Endo, Y. Aoyama, *Chem. Lett.* **2000**, 1424. b) T. Tanaka, T. Tasaki, Y. Aoyama, *J. Am. Chem. Soc.* **2002**, *124*, 12453.

21   T. Sawaki, T. Dewa, Y. Aoyama, *J. Am. Chem. Soc.* **1998**, *120*, 8539.

22   T. Sawaki, Y. Aoyama, *J. Am. Chem. Soc.* **1999**, *121*, 4793.

23   T. Dewa, T. Saiki, Y. Aoyama, *J. Am. Chem. Soc.* **2001**, *123*, 502.

24   For the catalytic performance of the La host in the Michael addition and (nitro) aldol reactions, see: T. Saiki, Y. Aoyama, *Chem. Lett.* **1999**, 797.

25   T. Dewa, Y. Aoyama, *J. Mol. Catal. A: Chem.* **2000**, *152*, 257.

26   Y. Aoyama, Y. Nagai, J. Otsuki, K. Kobayashi, H. Toi, *Angew. Chem., Int. Ed. Engl.* **1992**, *31*, 745.

27   K. Kobayashi, Y. Asakawa, Y. Kato, Y. Aoyama, *J. Am. Chem. Soc.* **1992**, *114*, 10307.

28   Y. Nagai, K. Kobayashi, H. Toi, Y. Aoyama, *Bull. Chem. Soc. Jpn.* **1993**, *66*, 2965.

29   T. Fujimoto, C. Shimizu, O. Hayashida, Y. Aoyama, *J. Am. Chem. Soc.* **1997**, *119*, 6676.

30   T. Fujimoto, C. Shimizu, O. Hayashida, Y. Aoyama, *J. Am. Chem. Soc.* **1998**, *120*, 601.

31   K. Fujimoto, T. Miyata, Y. Aoyama, *J. Am. Chem. Soc.* **2000**, *122*, 3558.

32   T. Fujimoto, C. Shimizu, O. Hayashida, Y. Aoyama, *Gazz. Chim. Ital.* **1997**, *127*, 5001.

33   O. Hayashida, K. Mizuki, K. Akagi, A. Matsuo, T. Kanamori, T. Nakai, S. Sando, Y. Aoyama, *J. Am. Chem. Soc.* **2003**, *125*, 594.

34   O. Hayashida, M. Kato, K. Akagi, Y. Aoyama, *J. Am. Chem. Soc.* **1999**, *121*, 11597.

35   Y. Aoyama, T. Kanamori, T. Nakai, T. Sasaki, S. Horiuchi, S. Sando, T. Niidome, *J. Am. Chem. Soc.* **2003**, *125*, 3455.

36   T. Nakai, T. Kanamori, S. Sando, Y. Aoyama, *J. Am. Chem. Soc.* **2003**, *125*, 8465.

37   S. Horiuchi, Y. Aoyama, *J. Controlled Release* **2006**, *116*, 107.

38   F. Osaki, T. Kanamori, S. Sando, T. Sera, Y. Aoyama, *J. Am. Chem. Soc.* **2004**, *126*, 6520.

39   K. Katagiri, R. Hamasaki, K. Ariga, J. Kikuchi, *J. Am. Chem. Soc.* **2002**, *124*, 7892.

40   K. Matsui, S. Sando, T. Sera, Y. Aoyama, Y. Sasaki, T. Komatsu, T. Terashima, J. Kikuchi, *J. Am. Chem. Soc.* **2006**, *128*, 3114.

41   Y. Sasaki, K. Matsui, Y. Aoyama, J. Kikuchi, *Nat. Protoc.* **2006**, *1*, 1227.

42   S. Sando, A. Narita, K. Abe, Y. Aoyama, *J. Am. Chem. Soc.* **2005**, *127*, 5300.

43   A. Narita, K. Ogawa, S. Sando, Y. Aoyama, *Angew. Chem., Int. Ed.* **2006**, *45*, 2879.

44   A. Narita, K. Ogawa, S. Sando, Y. Aoyama, *Nat. Protoc.* **2007**, *2*, 1105.

45   S. Sando, A. Narita, Y. Aoyama, *ChemBioChem* **2007**, *8*, 1795.

46   S. Sando, A. Narita, M. Hayami, Y. Aoyama, *Chem. Commun.* **2008**, 3858.

Yasuhiro Aoyama, born in 1945, received his Ph.D. from Kyoto University in 1974. He started his academic carrier in that year as a research associate in Kyushu University. After spending seven years in Kyushu University (research associate) and thirteen years in Nagaoka University of Technology as associate professor and full professor, he moved back to Kyushu University (Institute for Fundamental Research of Organic Chemistry) in 1995 and moved again to Kyoto University (Graduate School of Engineering) in 2001. His research areas have been diverse, covering bioorganic/inorganic chemistry, molecular recognition, structural organic chemistry, crystal engineering, catalysis, supramolecular chemistry, glycoscience and -technology, gene delivery and gene manipulation, chemical biology, and bioimaging. He received CSJ Award for Creative Work in 1991, Fluka Prize (Reagent of the Year) in 1993, Daily Niigata Cultural Award in 1993, and Chemical Society of Japan (CSJ) Award in 2006.